Chapter

Nanofibrous Scaffolds for Skin Tissue Engineering and Wound Healing Based on Nature-Derived Polymers

Lucie Bacakova, Julia Pajorova, Marketa Zikmundova, Elena Filova, Petr Mikes, Vera Jencova, Eva Kuzelova Kostakova and Alla Sinica

Abstract

Nanofibrous scaffolds belong to the most suitable materials for tissue engineering, because they mimic the fibrous component of the natural extracellular matrix. This chapter is focused on the application of nanofibers in skin tissue engineering and wound healing, because the skin is the largest and vitally important organ in the human body. Nanofibrous meshes can serve as substrates for adhesion, growth and differentiation of skin and stem cells, and also as an antimicrobial and moisture-retaining barrier. These meshes have been prepared from a wide range of synthetic and nature-derived polymers. This chapter is focused on the use of nature-derived polymers. These polymers have good or limited degradability in the human tissues, which depends on their origin and on the presence of appropriate enzymes in the human tissues. Non-degradable and less-degradable polymers are usually produced in bacteria, fungi, algae, plants or insects, and include, for example, cellulose, dextran, pullulan, alginate, pectin and silk fibroin. Well-degradable polymers are usually components of the extracellular matrix in the human body or at least in other vertebrates, and include collagen, elastin, keratin and hyaluronic acid, although some polymers produced by non-vertebrate organisms, such as chitosan or poly(3-hydroxybutyrate-*co*-3-hydroxyvalerate), are also degradable in the human body.

Keywords: skin replacements, wound dressings, nanofibers, electrospinning, epidermis, dermis, keratinocytes, fibroblasts, stem cells, vascularization, cell delivery, drug delivery, regenerative medicine

1. Introduction

Nanofibrous scaffolds are one of the most promising materials for skin tissue engineering and wound dressing, because they resemble nanoarchitecture of the native extracellular matrix (for a review, see [1]). Therefore, they can serve as suitable carriers of cells for tissue engineering and also as suitable wound dressings, which are able to protect the wound from external harmful effects, mainly

microbial infection, and at the same time, they can keep appropriate moisture and gas exchange at the wound site.

Nanofibrous scaffolds for skin tissue engineering have been fabricated from a wide range of synthetic and nature-derived polymers, which can be either biostable or degradable within the human body. Biostable synthetic polymers used in nanofiber-based skin regenerative therapies include, for example, polyurethane [2], polydimethylsiloxane [3], polyethylene terephthalate [4], polyethersulfone [5], and also hydrogels such as poly(acrylic acid) (PAA, [6]), poly(methyl methacrylate) (PMMA, [7]), and poly[di(ethylene glycol) methyl ether methacrylate] (PDEGMA, [8]). Degradable synthetic polymers typically include poly(ε-caprolactone) (PCL, [9]) and its copolymers with polylactides (PLCL, [10]), polylactides (PLA, [11]) and their copolymers with polyglycolides (PLGA, [12]), and also so-called auxiliary polymers, such as poly(ethylene glycol) (PEG), poly(ethylene oxide) (PEO, [13]) or poly(vinyl alcohol) (PVA, [14]), which facilitated the electrospinning process and improved the mechanical properties and wettability of the chief polymer. However, the synthetic polymers, although they are well-chemically defined and tailorable, are often bioinert, hydrophobic and thus not promoting cell adhesion, and also not well-adhering to the wound site. Therefore, they need to be combined with other bioactive substances, particularly nature-derived polymers.

This chapter is focused on nature-derived polymers used for fabrication of nanofibrous scaffolds for skin tissue engineering and wound healing. The advantages of most of these polymers are their better bioactivity, flexibility, wettability, and adhesion to the wound site. Similarly as synthetic polymers, also nature-derived polymers can be divided into polymers with none or limited degradability, when implanted into human tissues, and polymers well-degradable in human tissues. The first group includes glucans, such as cellulose, schizophyllan, dextran, starch, and other polysaccharides and proteins, such as pullulan, xylan, alginate, pectin, gum tragacanth, gum arabic, silk fibroin, and sericin. The second group of polymers degradable in human tissues includes collagen and its derivative gelatin, elastin, keratin, glycosaminoglycans such as hyaluronic acid, heparin and chondroitin sulfate, and also polymers not produced in the human body, namely chitosan, gellan gum, zein, and poly(3-hydroxybutyrate-*co*-3-hydroxyvalerate) (PHBV).

Some of the polymers degradable in human tissues, such as collagen, gelatin, elastin, keratin, and glycosaminoglycans, contain specific cell-binding motifs in their molecules, for example, specific amino acid sequences in proteins and oligosaccharide domains in glycosaminoglycans, which are recognized by cell adhesion receptors of integrin and non-integrin families (for a review, see [15, 16]). These molecules are often used in allogeneic or xenogeneic form, thus they can be associated with pathogen transmission or immune reaction. However, some synthetic polymers, for example PLA and PCL, have been reported to induce a more pronounced inflammatory reaction than gelatin [17].

This review chapter summarizes earlier and recent knowledge on skin tissue engineering and wound dressing applications, based on nanofibrous scaffolds made of nature-derived polymers, including our results.

2. Nature-derived nanofibers with none or limited degradability in the human tissues

Nature-derived nondegradable polymers or polymers with limited degradability in human tissues include polymers not occurring in the human body and synthesized by other organisms, such as plants, algae, fungi, insects, and bacteria.

Cellulose is a typical natural polymer nondegradable in human tissues. Cellulose belongs to the group of glucans, that is, polysaccharides derived from D-glucose, linked by glycosidic bond. In the cellulose molecules, these glycosidic bonds are of the β-type, thus the cellulose is a β-glucan. It is structural polysaccharide consisting of a linear chain of several hundred to over ten thousand β(1 → 4) linked D-glucose units. Cellulose is synthesized by plants, algae, fungi, some species of bacteria (*Gluconacetobacter xylinus*), and also by some animals, namely tunicates (*Styela clava*) (for a review, see [18, 19]).

Nanofibrous cellulose can be prepared in three basic forms: bacterial cellulose, which contains cellulose nanofibrils, synthesized by bacteria, nanofibrillar cellulose prepared from plants, particularly from wood, by hydrolysis, oxidation, and mechanical disintegration, and cellulose nanofibers created by electrospinning (for a review, see [19]). For electrospinning, cellulose should be solved. Well-known solvent of cellulose is N-methylmorpholine-N-oxide (NMMO). Another possibility is N-alkylinidazolium-derivate ionic liquid and N,N-dimethylacetamide containing 8 wt% of LiCl. However, any of them did not prove to be a good solvent for needleless electrospinning. The most favorable solvent of cellulose was found to be trifluoroacetic acid (TFA). However, TFA causes severe skin burns and is toxic for aquatic organisms even in low concentrations [20]. These problems, which limit the use of cellulose for creation of electrospun scaffolds for biomedical applications, can be solved by substituting the natural cellulose by its derivatives. The mostly used derivative of cellulose is cellulose acetate (CA), mainly due to its easier solubility and biocompatibility. CA can be dissolved in several solvents, however the best ones for electrospinning proved to be acetic acid (AA), and mixtures of acetone and N,N-dimethylacetamide (DMAC). Some results of successfully spun fibers by needleless electrospinning in our experiments can be found in **Figure 1**, demonstrating differences in the fiber morphology. The 95% aqueous mixture of AA showed the best results in comparison with acetone/DMAC mixtures due to production of smoother fibers and lower cytotoxicity.

All the mentioned forms of cellulose have been widely applied as wound dressings releasing various bioactive agents into wounds (antimicrobial, anti-inflammatory, antioxidative agents, cytokines, and growth and angiogenic factors), as transparent wound dressings for direct optical monitoring of wounds, for systemic

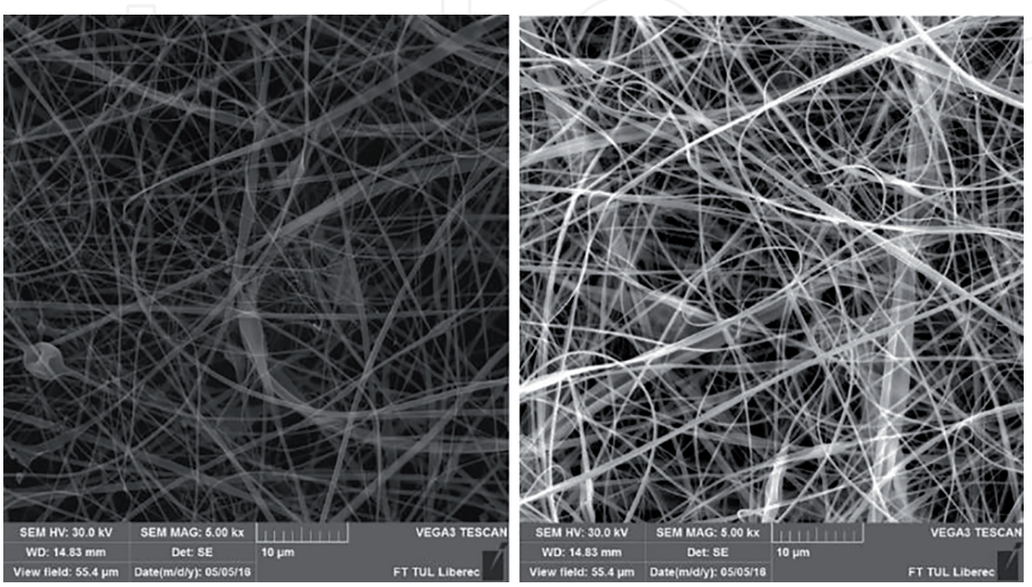

Figure 1.
Scanning electron microscopy of nanofibrous layers produced by wire needleless electrospinning using different solvents, namely 12 wt% of CA in acetone/DMAC (9:1) (left) or 14 wt% of CA in 95% AA (right).

transdermal drug delivery (analgesics, antiphlogistics, corticoids, and antihypertensives) and for construction of epidermal electronics for monitoring wound healing or physiological status of the organism. Non-degradable nanocellulose has also been used as a temporary carrier for delivery of keratinocytes, dermal fibroblasts, and mesenchymal stem cells into wounds (for a review, see [19]).

However, for use as direct scaffolds for skin tissue engineering, cellulose should be rendered degradable in human tissues. Cellulose is degradable by cellulase enzymes (exoglucanases and endoglucanases), which hydrolyze 1,4-beta-D-glycosidic linkages. These enzymes are not synthesized in human tissues, but they can be incorporated into cellulose scaffolds in order to degrade them gradually [21, 22]. These enzymes are believed to be non-toxic for mammalian cells [23, 24]. Moreover, the final product of cellulose degradation by these enzymes is glucose, which is a natural nutrient for the cells, by contrast with the acidic by-products of the standard currently used biodegradable PLA or PLGA scaffolds [25]. Another possibility how to use cellulase enzymes in skin tissue engineering (and in tissue engineering in general) is cell sheet technology. First, cells can be grown on the top of non-degradable cellulose substrates. After reaching the cell confluence, self-standing cell sheets can be released by exposure of the cellulose substrates to cellulases. Unlike the proteolytic enzymes conventionally used for detaching cells from their growth supports, cellulases do not disintegrate the extracellular matrix (ECM) formed by cells and do not cleave extracellular parts of cell adhesion receptors binding the ECM [26]. The cell sheets can be then replanted in the wound bed.

Another interesting approach how to render the cellulose degradable was metabolic engineering of *Gluconacetobacter xylinus*, which then produced modified cellulose molecules with intercalated N-acetylglucosamine (GlcNAc) residues, susceptible to degradation with lysozyme, present in the human body. After subcutaneous implantation in mice, the modified cellulose was completely degraded within 20 days [27, 28].

Other approaches how to render the cellulose degradable, at least partially, is its oxidation and other chemical modifications of cellulose, such as its conversion into regenerated cellulose or 2,3-dialdehydecellulose. In addition, cellulose of animal origin, that is, from tunicates, degraded more quickly than plant cellulose. For example, when cellulose films from *Styela clava* were implanted subcutaneously into rats for 90 days, they lost almost 24% of their initial weight, while the films prepared from wood pulp cellulose lost only less than 10% (for a review, see [19]).

Schizophyllan is another β-glucan used for potential wound healing application. It is an extracellular β-1,3 beta-glucan with β-1,6 branching, produced by the fungus *Schizophyllum commune*. In blends with PVA, it was used for electrospinning of nanofibrous scaffolds, which provided a suitable growth support for human dermal fibroblast. In experimental wound models *in vivo*, schizophyllan attracted macrophages, necessary for the first physiological phase of wound healing, that is, inflammation. Schizophyllan and other 1,3-β-glucans also increased collagen deposition, cellularity, formation of granulation tissue, and vascularity at the wound site [29].

Other glucans used for fabrication of nanofibrous scaffolds for skin tissue engineering and wound healing include dextran, starch and pullulan. According to the type of their glycosidic bonds, these polysaccharides belong to α-glucans.

Dextran is a branched complex glucan, in which the D-glucose units are linked by α-1,6 glycosidic bonds with branches from α-1,3 linkages. Dextran is of microbial origin; it can be produced, for example, by some lactic acid bacteria from sucrose. Dextran was used as a component of nanofibrous polyurethane-based wound dressings, in which dextran promoted neovascularization of the wound site, and also served as carrier for β-estradiol, an endogenous estrogen, a potent anti-inflammatory

agent, and mitogen for keratinocytes. In addition, the presence of dextran made the polyurethane dressing softer, more flexible, more wettable, and well-adherent to the wound and promoted hemostatic activity of the dressing. *In vitro*, the presence of dextran and β-estradiol enhanced the proliferation of 3T3-L1 fibroblasts on the scaffolds [30].

Dextran was also used as component of a bilayer scaffold for skin tissue engineering. The upper part of the scaffolds was made of electrospun blend of poly (ε-caprolactone-*co*-lactide) and poloxamer (i.e., Pluronic), and the lower part was made of a hydrogel composed of dextran and gelatin without the addition of a chemical crosslinking agent. The lower dextran/gelatin hydrogel layer provided a highly swollen three-dimensional environment similar to extracellular matrix (ECM) of soft tissues. Both part of the scaffolds supported the growth of adiposetissue-derived stem cells; however, the number of these cells on the hydrogels decreased with increasing content of dextran [31].

Dextran is degradable by dextranases, enzymes hydrolyzing (1 → 6)-alpha-D-glycosidic linkages. This enzyme is produced mainly by bacterial and fungi, but it was also detected in animal and human tissues, namely liver and spleen. Therefore, dextran is often chosen for biomedical applications, particularly drug delivery, because it is slowly degradable in human organism. Dextran molecules with Mw higher than 40 kDa are sequestered in the liver and spleen, and then hydrolyzed by endo- and exodextranases. Dextran molecules with Mw lower than 40 kDa can be eliminated through renal clearance [32]. However, dextran hydrogels implanted subcutaneously or intramuscularly into rats did not show signs of degradation 6 weeks post-implantation and were surrounded by a thin fibrous capsule and some macrophages and giant cells, which is a response typical for a number of non-degradable materials [32].

Starch is another α-glucan, containing both α-1,4- and α-1,6 glycosidic bonds. It serves an energy storage polysaccharide in plants, and from this point of view, it is considered to be an analogue of glycogen, energy storage polysaccharide in animals. Starch consists of two types of molecules, namely linear amylose and branched amylopectin (for a review, see [33]). Electrospun starch-based nanofibrous meshes were proposed for wound healing applications. The electrospinning of starch was facilitated by addition of PVA, that is, a noncytotoxic, water-soluble, biocompatible synthetic polymer which reduced the repulsive forces produced in starch solution. The scaffolds then promoted the proliferation of mouse L929 fibroblasts [34]. Starch is degradable by amylases, that is, hydrolases that act on α-1,4-glycosidic bonds. Amylases occur in three forms, namely α-, β-, and γ-amylases. These enzymes are synthesized by microorganisms (bacteria and fungi), plants, and with exception of β-amylases, also in animals. Alpha-amylases are present in human organism, but not currently in all tissues-they are important enzymes of gastrointestinal tract and are produced by salivary glands and pancreas. Interestingly, α-amylases were also found in brain, and their lower expression there is probably associated with the pathogenesis of Alzheimer's neurodegenerative disease [35].

Pullulan is also an α-glucan with both α-1,4- and α-1,6 glycosidic bonds. It is a linear polysaccharide consisting of maltotriose units, in which three glucose units in maltotriose are connected by an α-1,4 glycosidic bond, whereas consecutive maltotriose units are connected to each other by an α-1,6 glycosidic bond. Pullulan is produced from starch by the fungus *Aureobasidium pullulans*. It shows a high water-absorbing capability, adhesive properties, and the capability to form strong resilient films and fibers. It is degradable by pullulanase, a specific kind of glucanase, produced in bacteria and not present in human tissues. When pullulan hydrogels alone or in combination with dextran were implanted subcutaneously into rats, they induced inflammatory reaction and were surrounded by a fibrous capsule [36]. Nevertheless, pullulan is water-soluble and thus removable from human issues, and

in combination with chitosan and tannic acid, it was used for fabrication of electrospun nanofibrous meshes promising for wound healing [37]. In combination with dextran and gelatin, pullulan was used for electrospinning of nanofibrous scaffolds promising for skin tissue engineering. These scaffolds, especially when crosslinked with trisodium trimetaphosphate, supported the adhesion and spreading of human dermal fibroblasts and formation of actin cytoskeleton in these cells [38].

Xylan is a plant polysaccharide belonging to the group of hemicelluloses, that is, polymers often associated with cellulose. While cellulose is made of glucose units, hemicelluloses contain many different sugar monomers. Xylans are polysaccharides made of β-1,4-linked xylose (i.e., a pentose sugar) residues with side branches of α-arabinofuranose and α-glucuronic acids, which contribute to crosslinking of cellulose microfibrils and lignin through ferulic acid residues. Xylans are considered as relatively available and cost-effective natural materials for tissue engineering. Electrospun nanofibers containing beech-derived xylan and PVA were tested as potential dermal substitutes for skin tissue regeneration. These scaffolds provided a good support for the adhesion and proliferation of human foreskin fibroblasts and for production of collagen by these cells [39]. Bagasse xylan was also a component of hydrogels endowed with shape memory, namely carboxymethyl xylan-g-poly(acrylic acid) hydrogels, applicable in tissue engineering and biosensorics, particularly for construction of electronic skin [40].

Alginates, for example, sodium alginate or calcium alginate, are salts of alginic acid, a linear polysaccharide composed of (1,4)-β-D-mannuronic acid and (1,3)-α-L-guluronic acid. Alginates are produced by various species of brown algae, and also by the bacterium *Pseudomonas aeruginosa*, a major pathogen found in the lungs of patients with cystic fibrosis. The structure of alginates is similar to glycosaminoglycans, an important component of ECM in human tissues including skin [41]. Alginates have a great ability to keep moisture in the wound site and to adhere to skin. However, alginates are poorly spinnable, and therefore, for skin tissue engineering and wound dressing applications, they were electrospun together with other polymers, such as PVA [41, 42] or PEO [43]. Poor mechanical properties of alginates have been compensated by the combination with chitosan [44] or PCL [44, 45]. In addition, alginates themselves are not adhesive for mammalian cells, which was compensated by their combination with collagen and gelatin, containing ligands for cell adhesion receptors [41]. Alginates were modified with a cell adhesive GRGDSP oligopeptide, which acts as ligand for integrin cell adhesion receptors [43]. Sodium alginate was used for attachment of arginine to the surface of chitosan nanofibers in order to increase healing capability of this wound dressing [46]. Alginate nanofibers supported by PCL were impregnated with an extract from *Spirulina*, a photosynthetic cyanobacterium producing bioactive molecules with anti-oxidant and anti-inflammatory effects [45]. Electrospun sodium alginate nanofibers containing silver nanoparticles were used for fabrication of an electronic skin capable of pressure sensing and endowed with antibacterial activity [47].

The degradability of alginate in human organism is limited. Alginate is naturally degraded by alginate lyases or alginate depolymerases, which have been isolated from marine algae, marine animals, bacteria, fungi, viruses, and other microorganisms, but are not present in the human organism. Degradability of alginate can be increased by its oxidation and at low pH. Also the hydrophilicity and water uptake capacity of alginate can help in its removal from the wound site (for a review, see [48]).

Pectin is a complex of structural polysaccharides present in the cell walls of terrestrial plants, rich in galacturonic acid. Pectin is known as gelling agent in food industry, but it is also widely used in medicine, for example, against digestive disorders, such as obstipation and diarrhea, for oral drug delivery, as a component of dietary fibers trapping cholesterol and carbohydrates, as a demulcent, that is, a

mucoprotective agent, and also in wound healing preparations [49]. Pectin is known as a natural prophylactic substance against poisoning with toxic cations, and its hemostatic and curing effects are well-documented in healing ointments [50]. Pectin is degradable by enzymes produced by bacterial, fungal and plant cells, and not present in human tissues [51–53]. Thus, pectin is degradable, at least partly, only in the intestinal tract populated with bacteria. However, pectin is water-soluble and quickly dissolves in the water environment, including the tissues. Therefore, in order to increase its stability, it was combined with chitosan and TiO_2 nanoparticles for wound dressing applications [50] or used for construction of composite chitosan-pectin scaffolds for skin tissue engineering. Blending chitosan with pectin markedly improved the mechanical properties of the scaffolds, such as their Young's modulus, strain at break and ultimate tensile strength, in comparison with pure chitosan scaffolds, although the proliferation of cells (i.e., fibroblasts) was slightly slower on pectin-containing scaffolds [54, 55]. The reason is that pectin does not contain cell binding domains. The cell adhesion on pectin nanofibers was markedly enhanced by oxidizing pectin with periodate to generate aldehyde groups, and then crosslinking the nanofibers with adipic acid dihydrazide to covalently connect pectin macromolecular chains with adipic acid dihydrazone linkers. In addition, the crosslinked pectin nanofibers exhibited excellent mechanical strength and enhanced body degradability [56].

Other polysaccharides explored for creation of nanofibrous scaffolds for skin tissue engineering and wound healing are gum tragacanth and gum arabic, both polysaccharides of plant origin, degradable by bacteria and fungi, for example, in soil [57, 58].

Gum tragacanth is a viscous water-soluble mixture of polysaccharides, mainly tragacanthin and bassorin. Tragacanthin dissolves to give a colloidal hydrosol. Bassorin, representing 60–70% of the gum, is insoluble and swells to a gel. Chemically, tragacanthin is a complex mixture of acidic polysaccharides containing D-galacturonic acid, D-galactose, L-fucose (6-deoyl-L-galactose), D-xylose, and L-arabinose. Bassorin is probably a methylated tragacanthin. A small amount of cellulose, starch, protein and ash are also present (https://colonygums.com/tragacanth). In order to improve electrospinning and mechanical properties of the gum tragacanth, it was combined with PVA and PCL [59]. Gum tragacanth is endowed with microbial resistance and wound healing activity, which was further enhanced by curcumin, a naturally occurring poly-phenolic compound with a broad range of favorable biological functions, including anti-cancer, anti-oxidant, anti-inflammatory, anti-infective, angiogenic, and healing properties [60].

Gum arabic, also known as gum acacia, is a complex and water-soluble mixture of glycoproteins and polysaccharides consisting mainly of arabinose and galactose. For skin tissue engineering, it was electrospun with PCL and also with zein, a storage plant protein [61].

Silk fibroin is a water-insoluble elastic protein present in silk fibers produced by larvae of *Bombyx mori* and some other moth of the *Saturniidae* family, such as *Antheraea assama, Antheraea mylitta*, and *Philosamia ricini* [62–64]. Silk fibroin occurs in the fibers together with sericin, a water-soluble serine-rich protein, which forms a glue-like layer coating two singular filaments of fibroin.

In biomaterial science, silk fibroin is considered to be degradable, but in mammalian organism, this degradation is long-lasting and can take more than 1 year. As a kind of biomaterial approved by the Food and Drug Administration (FDA) for medical use, silk is defined by United States Pharmacopeia as non-degradable for its negligible tensile strength loss *in vivo*. However, silk fibroin is susceptible to biological degradation by proteolytic enzymes such as chymotrypsin, actinase, carboxylase, proteases XIV, XXI and E, and collagenase IA. The final degradation products of silk fibroin are amino acids, which are easily absorbed *in vivo* (for a review, see [65]).

The degradation behavior of fibroin scaffolds depends on the preparation method and structural characteristics, such as processing condition, pore size, and silk fibroin concentration (for a review, see [65]). For example, three-dimensional porous scaffolds prepared from silk fibroin using all-aqueous process degraded within 2–6 months after implantation into muscle pouches of rats, while the scaffolds prepared using an organic solvent, hexafluoroisopropanol (HFIP), persisted beyond 1 year. It was probably due to a lower original silk fibroin concentration, larger pore size, and a higher and more homogeneous cellular infiltration of aqueous-derived scaffolds than in HFIP-derived scaffolds [66].

For skin tissue engineering and wound healing, silk fibroin has been combined with various synthetic and natural polymers and other bioactive substances. The polymers included, for example, PCL, [67], poly(L-lactic acid)-*co*-poly(ε-caprolactone) (PLACL, [68]), carboxyethyl chitosan, PVA, [69], chitin [70], cellulose-based materials modified by oxidation [71] or with lysozyme [72], collagen [73], gelatin [74], and hyaluronan [75]. The bioactive substances were, for example, growth factors, such as epidermal growth factor [64], vitamins, such as vitamin C [68], vitamin E [76], and pantothenic acid (vitamin B5; [77]), antioxidants, such as grape seed extract ([78]) or quinone-based chromenopyrazole [79], antibiotics, such as ciprofloxacin [64], tetracycline [68] or gentamycin [62], and other antimicrobial and wound healing agents, such as silver nanoparticles, dandelion leaf extract [63], *Aloe vera* [80], or astragaloside IV [74]. In order to enlarge the pore size in nanofibrous scaffolds for cell penetration, silk fibroin was electrospun together with so-called "sacrificial" crystals of ice [67] or NaCl [81, 82], that is, crystals which are removed after the electrospinning process. An interesting combination is silk fibroin with decellularized human amniotic membrane, which was used for developing a three-dimensional bi-layered scaffold for burn treatment. Adipose tissue-derived mesenchymal stem cells seeded on this scaffold increased expression of two main pro-angiogenesis factors, vascular endothelial growth factor, and basic fibroblast growth factor [83]. Also the transplantation of bone marrow-derived mesenchymal stem cells and epidermal stem cells into wounds using nanofibrous silk fibroin scaffolds supported re-epithelization, collagen synthesis, as well as the skin appendages regeneration [84]. Another interesting approach is to use silk fibroin produced by other species than *Bombyx mori*, namely by the moths *Antheraea assama* and *Philosamia ricini*. This "non-mulberry" silk fibroin possesses inherent Arg-Gly-Asp (RGD) motifs in its protein sequence, which facilitates binding of cells through their integrin adhesion receptors [64].

Sericin has also been applied in skin tissue engineering and wound healing, although in a lesser extent than silk fibroin. Sericin shows antioxidant, UV-protective, heat-protective, moisture-retaining, and antimicrobial properties, which have been reported to be more pronounced in non-mulberry sericin (e.g., from *Antheraea mylitta*) than in sericin produced by *Bombyx mori*. The reason is that wild moths like *Antheraea mylitta* are exposed to a hostile environment in nature than *Bombyx mori* raised in captive conditions. Similarly as non-mulberry silk fibroin, also sericin has been reported to be more supportive for cell adhesion than mulberry sericin (for a review, see [85]). Sericin enhanced the proliferation and epidermal differentiation of human mesenchymal stem cells on gelatin/hyaluronan/chondroitin sulfate nanofibrous scaffolds [86]. Similarly, sericin improved the growth of murine L929 fibroblasts and human HaCaT keratinocytes cultured on the PVA nanofibrous scaffolds [87] and also the growth of L929 fibroblasts on chitosan nanofibrous scaffolds, together with antibacterial properties of these scaffolds [88].

3. Nature-derived nanofibers degradable in the human tissues

Nature-derived polymers degradable in human tissues include, in particular, polymers that are synthesized in the human body and usually act as components of ECM. These polymers are proteins (collagen and its derivative gelatin, elastin, fibrinogen and fibrin, keratin) or polysaccharides in non-sulfated form (hyaluronic acid) and sulfated form (heparin-like glycosaminoglycans). In addition, some natural polymers synthesized by other organisms, such as bacteria, fungi, insects, crustaceans or plants, are degradable in human tissues, because they are susceptible to enzymes present in human tissues, such as lysozyme and esterases. These polymers include chitosan, gellan gum, zein, and PHBV.

Collagen is the main structural protein in the extracellular space in a wide range of tissues in the body. Skin contains type I collagen, one of the most abundant collagens in the human body. Type I collagen is also abundant in tendons, ligaments, and vasculature, and it is a main component of the organic part of bone. Type I collagen is a fibrillar type of collagen; it is composed of amino acid chains forming triple-helices of elongated fibrils. That is why the nanofibrous collagen scaffolds closely mimic the architecture of the native ECM and are advantageous for tissue engineering. In addition, collagen has been reported to be relatively poorly immunogenic, even if used in allogeneic and xenogeneic forms, for example, recombinant human collagen or bovine and porcine collagen. However, mammalian collagen is associated with the risk of disease transmission, for example, bovine spongiform encephalopathy (for a review, see [89–91]). This risk can be reduced by the use of fish collagen, which became to be popular in tissue engineering, including skin tissue engineering and wound healing. In addition, the fish collagen enables an easier recovery of intact collagen triple helices than the mammalian collagen [92]. Fish collagen can be obtained from the skin, scales and bones of freshwater fish, such as tilapia [91–94], and marine fish, such as hoki fish (*Macruronus novaezelandiae*) [92, 95], or *Arothron stellatus,* also known as "stellate puffer," "starry puffer" or "starry toadfish" [96]. Nanofiber electrospun from tilapia skin collagen promoted the proliferation of human HaCaT keratinocytes, and stimulated epidermal differentiation through the up-regulated gene expression of involucrin, filaggrin, and type I transglutaminase in these cells. Moreover, the tilapia collagen nanofibers accelerated wound healing *in vivo* in rat models [91–94]. Beneficial effects on wound healing were also observed in nanofibrous meshes electrospun from collagen obtained from *Arothron stellatus* [96] and from fish scale collagen peptides [90].

Collagen is one of the most widely used natural proteins for creation of nanofibrous scaffolds for skin tissue engineering and wound healing. However, these scaffolds are usually mechanically weak, and therefore they need crosslinking or blending with synthetic polymers. Collagen crosslinking with conventionally used agents, particularly glutaraldehyde, is associated with the risk of the scaffold cytotoxicity. More benign crosslinkers used recently include, for example, citric acid [95] or quaternary ammonium organosilane, a multifunctional crosslinking agent, which improved the electrospinnability of collagen by reducing its surface tension, endowed the collagen nanofibers with potent antimicrobial activity and promoted the adhesion and metabolic activity of primary human dermal fibroblasts without any cytotoxicity, at least in a lower concentration of 0.1% w/w [97].

Synthetic polymers used for combination with collagen in nanofibrous scaffolds included PLA [98], PLGA [99, 100], and particularly PCL, which was either blended with collagen [101–104] or served as substrate for subsequent deposition of collagen [105]. Collagen has also been combined with natural polymers, such as silk fibroin [73] or chitosan in a form of blends [106] or in a form of bilayered scaffolds, where collagen was electrospun onto the chitosan scaffolds [107]. Collagen was also

grafted on the surface of composite electrospun PVA/gelatin/alginate nanofibers [41]. Collagen-based or collagen-containing nanofibers have been loaded with a wide range of bioactive substances, such as vitamin C, vitamin D3, hydrocortisone, insulin, triiodothyronine, and epidermal growth factor [100], transforming growth factor-β1 [102], plant extracts such as *Coccinia grandis* leaf extract [96], or lithospermi radix extract [107], antibiotics such as gentamicin [103], or bioactive glass [93, 104]. Collagen and PCL and bioactive glass nanoparticles were applied for delivery of endothelial progenitor cells into wounds in order to promote their vascularization and healing [104].

Gelatin is a derivative of collagen, obtained by denaturing its triple helical structure. Specifically, it is a mixture of peptides and proteins produced by partial hydrolysis of collagen extracted from the skin, bone, and connective tissue of animals, such as cattle, pigs, chicken, and also fish. Gelatin can be defined as a complex mixtures of oligomers of the α subunits joined by covalent bonds, and intact and partially hydrolyzed α-chains of varying molecular weight (for a review, see [89, 92]). Properties of gelatin, including its spinnability, depend on the source of collagen, animal species, age, type of collagen, type of conversion of collagen to gelatin (i.e., acidic *vs.* basic hydrolysis), and particularly on the conformation of gelatin molecules [108].

Similarly as collagen, also gelatin is the most promising for skin tissue engineering and wound healing applications in combination with various synthetic and natural polymers. For example, gelatin was combined with polyurethane [109], PLA [11, 17], and particularly with PCL, where it was incorporated into core-shell PCL/gelatin nanofibers as the core polymer [110] or electrospun independently of PCL using a double-nozzle technique, which resulted in creation of two types of nanofibers in the scaffolds, either mixed [111] or arranged in separate gelatin and PCL layers [112]. Gelatin was also combined with a copolymer of lactic acid and caprolactone P(LLA-CL) in the form of blends [113] or in the form of coaxial nanofibers with P(LLA-CL)/gelatin shell and albumin core containing epidermal growth factor, insulin, hydrocortisone, and retinoic acid [114]. Natural proteins combined with gelatin included dextran [31], pullulan [38], alginate [41], silk fibroin [74], and hyaluronan with chondroitin sulfate [86].

For combination with synthetic and natural polymers, for example, with PCL [115], and chitosan and keratin [116], gelatin was also used in the form of photocrosslinkable gelatin methacrylate hydrogel (GelMA). On PCL nanofibers, GelMA showed a higher decoration level in comparison with native gelatin [116]. Self-standing nanofibrous matrices electrospun from GelMA enabled tuning of their water retention capacity, stiffness, strength, elasticity, and degradation by changing the exposure time to UV light [117].

Elastin is a protein found in the ECM, that maintains its elasticity [118]. It is the second main protein-based component of native skin ECM. The presence of elastin in composite electrospun nanofibrous scaffolds, containing gelatin, cellulose acetate and elastin, changed the fiber morphology from straight to ribbon-like structure, and decreased the swelling ratio and degradation rate of the scaffolds. In addition, elastin-containing scaffolds supported the attachment and proliferation of human fibroblasts [119].

Fibrin is a provisional ECM protein, which accumulates in wounds after injury to initiate hemostasis and healing. Fibrin is formed via the polymerization of fibrinogen monomers in the presence of thrombin, and this process can be simulated *in vitro* [120]. Fibrin forms a fine nanofibrous mesh, which is mechanically weak and needs to be deposited on some supportive structure, for example, synthetic nanofibrous meshes made of poly(L-lactide) (PLLA) [121]. In our experiments, fibrin was deposited on PLLA in the form of two types of coating, depending on the mode of

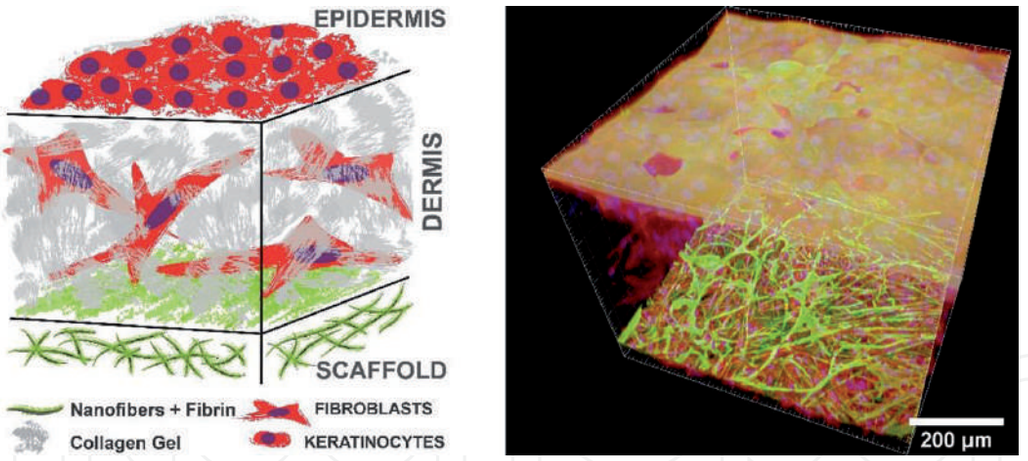

Figure 2.
Developing a bilayer construct of keratinocytes and fibroblasts on a PLLA nanofibrous membrane with fibrin and collagen hydrogel. Left: schematic design; right: real construct.

fibrin preparation. Fibrin either covered the individual fibers in the membrane (F1 nanocoating), or covered the individual fibers and also formed a fine homogeneous nanofibrous mesh on the surface of the membrane (F2 nanocoating), depending on the mode of fibrin preparation. The fibroblasts on the F1 nanocoating remained in their typical spindle-like shape, while the cells on the F2 nanocoating were polygonal with a higher proliferation rate [122]. F2 nanocoating was then used for development of a bilayer skin construct. First, a nanofibrous PLLA mesh was coated with fibrin and seeded with human dermal fibroblasts. After reaching confluence, the fibroblasts were covered with a collagen hydrogel and were allowed to migrate into this hydrogel and to proliferate inside. After sufficient colonization of the hydrogel with fibroblasts and formation of a structure resembling the skin dermis, human epidermal keratinocytes were seeded on the top of the collagen hydrogel (**Figure 2**) [123].

Also fibrinogen was used for modification of synthetic polymeric nanofibers in order to enhance the cell adhesion and growth. Nanofibrous scaffolds electrospun from blends of PCL and fibrinogen improved the adhesion, proliferation, and epidermal differentiation of adipose tissue-derived stem cells (ADSCs) in comparison with pure PCL scaffolds. Composite PCL/fibrinogen scaffolds seeded with ADSCs also markedly improved healing of full-thickness excisional wounds created in rats in comparison with acellular dermal matrix or acellular dermal matrix with ADSCs [124].

Keratin is a fibrous structural protein, present in skin appendages, such as hair, wool, feather, nails, horns, claws, hooves, and in the outer (cornified) layer of epidermis [125, 126]. Keratin protects epithelial cells from damage and stress and is insoluble in water and organic solvents.

In most studies dealing with keratin-containing nanofibers, keratin was combined with other natural or synthetic polymers in order to improve the spinnability of keratin, or to improve the bioactivity of the co-electrospun polymer. For example, in a study by Cruz-Maya *et al*. [127], blending keratin with PCL improved the stability of the electrospinning process, promoted the formation of nanofibers without defects, such as beads and ribbons, typically observed in the fabrication of keratin nanofibers. At the same time, keratin markedly increases the fiber hydrophilicity compared with pure PCL, which improved the adhesion and proliferation of human mesenchymal stem cells [127]. Similarly, co-electrospinning of keratose (i.e., oxidative keratin) with PVA resulted in nanofibers with uniform fibrous structure, suitable hydrophilicity and mechanical properties [125]. Properties of electrospun keratin nanofibers were also improved by incorporation of hydrotalcites, intended for delivery of diclofenac. These nanofibers displayed a reduced swelling

ratio and a slower degradation profile compared to keratin-based non-woven nanofibrous mats containing free diclofenac [126]. Keratin was also a component of core-shell nanofibers, prepared by coaxial electrospinning of chitosan, PCL and keratin with *Aloe vera* extracts encapsulated inside the polymer nanofibers. This construct increased the adhesion and growth of L929 fibroblasts and was intended for wound healing applications [128]. Importantly, keratin was a component of bilayer scaffolds for skin tissue engineering, composed of human hair keratin/chitosan nanofiber mat and gelatin methacrylate (GelMA) hydrogel. Human dermal fibroblasts were encapsulated and grown in the hydrogel matrix, while human HaCaT keratinocytes formed a layer on the top of the scaffolds, mimicking dermis and epidermis of skin tissue [116]. Another bilayer scaffolds was constructed using polyurethane wound dressing as an outer layer, and electrospun gelatin/keratin nanofibrous mat as an inner layer [109].

Hyaluronic acid, also called hyaluronan, is an anionic, non-sulfated linear glycosaminoglycan. It is distributed widely throughout connective, neural, and epithelial tissues, including skin, where it is a major component of ECM. Therefore, hyaluronic acid has been widely used for skin tissue engineering and wound healing, and it is approved for clinical application [33].

Hyaluronic acid stimulated infiltration of nanofibrous scaffold composed of hyaluronan, silk fibroin and PCL [75], and can help to promote cell proliferation [129]. Electrospinning of pure hyaluronic acid is not simple because of solubility characteristics of this polymer. Hyaluronic acid is well-soluble in water but less-soluble in most organic solvents, which can be solved by mixtures of solvents as water/ethanol or water/dimethylformamide [130]. Increasing of evaporation and decreasing of solution surface tension by the solvent mixing helps to electrospinning process. Another possibility is electrospinning of hyaluronic acid together with a suitable water-soluble polymer such as PVA [131] or PEO. The solution of pure hyaluronic acid [132] or with relatively small amount of carrier PEO was successfully spun into nanofibrous material by air-assisted electrospinning technology, that is, electroblowing [133]. For creation of nanofibrous scaffolds, hyaluronic acid was also used in combination with PCL [134], PLA [135] or gelatin, chondroitin sulfate and sericin [86].

Sulfated glycosaminoglycans have been relatively rarely used as components of nanofibers for skin tissue engineering and wound healing in comparison with hyaluronic acid. This group of polysaccharides include heparin, heparan sulfate, chondroitin sulfate, dermatan sulfate, and keratan sulfate (for a review, see [33]). From these polysaccharides, only heparin, heparan sulfate, and chondroitin sulfate were used as components of nanofibers for skin regenerative therapies. For example, heparin coatings on PLLA nanofibers increased the infiltration of the scaffolds with endothelial cells *in vitro,* and enhanced epidermal skin cell migration across the wound in a full-thickness dermal wound model in rats *in vivo* [136]. In a recent study by Yergoz *et al*. [137], a heparin-like nanofibrous hydrogel promoted regeneration of full thickness burn injury in mice. Chondroitin sulfate was used as a component of electrospun gelatin/PVA/chondroitin sulfate nanofibrous scaffolds, which supported the proliferation of human dermal fibroblasts [138], of electrospun nanofibrous composite scaffolds made of cationic gelatin/hyaluronan/chondroitin sulfate loaded with sericin, which promoted the differentiation of human mesenchymal stem cells toward epithelial lineage [86], and of electrospun gelatin/chondroitin sulfate nanofibrous scaffolds, which accelerated healing of full-thickness skin excision wounds in rats [139].

Chitosan is a linear polysaccharide composed of randomly distributed β-(1 → 4)-linked D-glucosamine (deacetylated unit) and N-acetyl-D-glucosamine

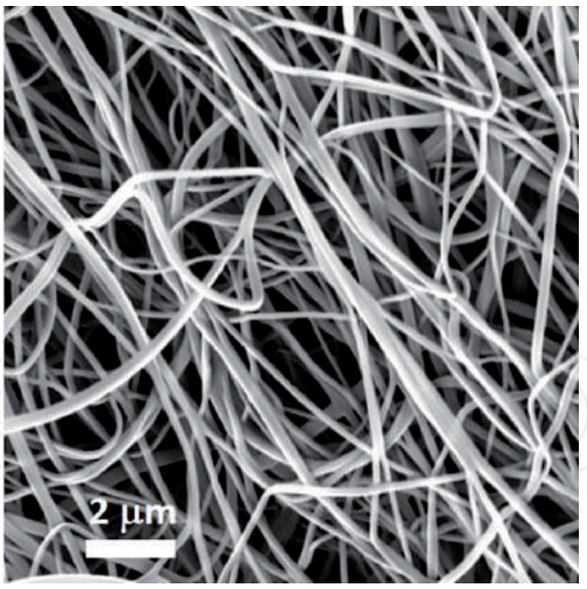

Figure 3.
Scanning electron microscopy of nanofibrous layers produced by needle electrospinning from PVA/chitosan solution.

(acetylated unit). It can be prepared by alkali treatment from chitin, a poly-N-acetyl-D-glucosamine polysaccharide, the major structural component of the exoskeleton of crustaceans (crab, shrimp), and of the cell wall of fungi and yeast [140]. Chitosan is known as biocompatible, antimicrobial, and biodegradable. In the human organism, it can be degraded by lysozyme, a hydrolytic enzyme present in various secretions such as saliva, tears, mucus, and human milk, and also in cytoplasmic granules of macrophages and polymorphonuclear neutrophils. Chitosan breakdown by lysozymes happens via the removal of glycosidic bonds between polysaccharide units in the polymer. Glucosamine and saccharide are the products of this process, which can be metabolized or stored as proteoglycans in the body.

However, electrospinning of chitosan is difficult due to its polycationic characters. Due to the presence of amine groups in the chitosan molecule, acidic aqueous solutions are the best solvents for this polymer. The best candidates for solvent system seem to be mixture of acetic acid (AA) and formic acid (FA) or trifluoroacetic acid (TFA); however, TFA is highly toxic. Electrospinning of pure chitosan has very low productivity because it requires very concentrated polymeric solutions [141]. Therefore, for creation of nanofibrous scaffolds for skin tissue engineering, chitosan has been mixed with other natural or synthetic polymers, such as collagen [142], gelatin [143], keratin [116], cellulose [144], pectin [54, 55], silk fibroin [69], PHBV [145], PCL [142], PLA [146], PLGA [147], PEO, [148], and also with PVA, which was used in our studies (**Figure 3**). Chitosan has also been mixed with various nanoparticles, such as halloysite nanotubes [149], graphene oxide [150] or nanodiamonds [144]. The reason of all these mixtures was to improve the stability, spinnability, wettability, mechanical properties, and biofunctionality of chitosan-containing scaffolds for skin tissue engineering. Combination of chitosan with various polymers also enabled creation of bilayer scaffolds for reconstruction of two main skin layers, that is, epidermis containing keratinocytes and dermis containing fibroblasts [116, 142]. In order to enhance the antimicrobial and wound healing activity of chitosan, this polymer was electrospun together with extract from Henna leaves [151]. In addition, chitosan nanoparticles have been incorporated in nanofibrous scaffolds as carriers for controlled drug delivery, for example, delivery of growth factors, cytokines and angiogenic factors, such as platelet-derived growth factor [152], granulocyte colony-stimulating factor [153] or angiogenin [147].

Nanofibrous scaffolds promising for skin tissue engineering and wound healing were also prepared directly from chitin, which was electrospun either alone with further modifications with fibronectin, laminin and particularly with type I collagen [154], or in combination with silk fibroin [70].

Gellan gum is a water-soluble anionic polysaccharide produced by the bacterium *Sphingomonas elodea* (formerly *Pseudomonas elodea*). The repeating unit of the polymer is a tetrasaccharide, which consists of two residues of D-glucose, one of residue of L-rhamnose and one residue of D-glucuronic acid. For skin tissue engineering and wound healing, gellan gum was electrospun with PVA in order to decrease its viscosity and repulsive forces between the polyanions along the polymer chains and to increase the stability, uniformity, and structural consistency of the nanofibers in aqueous environment. The nanofibrous scaffolds were further stabilized by crosslinking with various physical, chemical, and ionic methods, such as by heat, UV irradiation, methanol, glutaraldehyde, and by calcium chloride [155]. These scaffolds supported the adhesion and growth of human dermal 3T3-L1 fibroblasts [155, 156] and human HaCaT keratinocytes [157] and provided a better support for these cells than conventionally proposed gellan-based hydrogels and dry films. In addition, these scaffolds were endowed with antimicrobial activity by incorporation with amoxicillin, and accelerated healing of full-thickness skin excision wound in rats in comparison with non-treated wounds [157]. Similarly as chitosan, gellan gum has been reported to be degradable by lysozyme [158]. Three-dimensional printed gellan gum scaffolds also showed degradation *in vitro* in phosphate-buffered saline (PBS) or in simulated body fluid, and the degradation rate could be modulated by changing the ratio of surface area per mass of the scaffolds [159].

Zein is the major storage protein of corn, composed of amino acids such as leucine, glutamic acid, alanine and proline, and showing good biocompatibility, flexibility, microbial resistance, and antioxidant activity [61]. Zein has been shown to degradable *in vitro* in PBS and also *in vivo* when implanted subcutaneously in rats in the form of rod-like implants [160]. However, similarly as in many other natural polymers, the application of pure zein nanofibers is limited because of poor mechanical properties of these fibers. Therefore, for skin tissue engineering and wound dressing applications, zein has been mixed with various synthetic and nature-derived polymers, such as polyurethane [161], PLA [162], PCL, hyaluronic acid, chitosan [163], and polydopamine [164], and impregnated with TiO_2 nanoparticles [164] or Ag nanoparticles [161] in order to enhance the antimicrobial activity of the scaffolds.

Poly(3-hydroxybutyrate-co-3-hydroxyvalerate) (PHBV), is a polymer produced naturally by bacteria as a storage compound under growth-limiting conditions. It is a thermoplastic linear aliphatic polyester of polyhydroxyalkanoate type. PHBV is approved by the FDA for medical use. PHBV is biodegradable by bacterial enzymes, but it is also susceptible to hydrolytic degradation in water environment, although this degradation is relatively slow. When degradation of porous PHBV scaffolds for tissue engineering was simulated *in vitro* in PBS at 37°C, it lasted several months [165]. In the human body, however, the degradation of PHBV can be accelerated by nonspecific esterase and lysozyme enzymes, both present in cells of the immune system (for a review, see [165]). For biomedical application, PHBV is often used as an alternative to synthetic polymers, but it has several drawbacks, such as relatively high cost, brittleness, relatively difficult processing, and also hydrophobicity, which can hamper the cell adhesion and growth. However, PHBV is piezoelectric, which can stimulate the adhesion, growth, and phenotypic maturation of cells. Pure electrospun PHBV meshes supported the adhesion, growth, and epidermal differentiation of bone marrow mesenchymal stem cells, which was induced by an appropriate composition of cell culture media, containing epidermal

growth factor, insulin, 3,3′,5-triiodo-L-thyronine (T3), hydrocortisone, and 1α, 25-dihydroxyvitamin (D3), and manifested by expression of genes for keratin, filaggrin, and involucrin, that is, an early, intermediate and late marker of keratinocyte differentiation, respectively [166]. In order to increase the attractiveness of electrospun PHBV nanofibers for the cell adhesion and growth, they were coated with collagen [167] blended with collagen [168], blended with chitosan [145] or blended with keratin [169]. Collagen-coated PHBV nanofibers alone or seeded with unrestricted somatic stem cells, isolated from umbilical cord, accelerated closure of excision wounds in rats *in vivo* compared to unmodified PHBV nanofibers [167]. Similar wound healing effect was also obtained with PHBV nanofibers blended with keratin [169]. Mechanical properties of PHBV nanofibers were improved by addition of graphene oxide nanoparticles in the electrospinning solution, which also endowed these fibers with and antimicrobial activity [167].

4. Conclusions

Nanofibrous scaffolds made of nature-derived polymers hold a great promise for skin tissue engineering and wound healing. These scaffolds are created from biological matrices, and from this point of view, they resemble the extracellular matrix more closely than synthetic polymers. Some of these polymers, such as collagen, gelatin, elastin, keratin, nonsulfated and sulfated glycosaminoglycans, and also nonmulberry silk fibroin, contain motifs that are recognized and bound by cell adhesion receptors. Therefore, nature-derived polymers can increase the bioactivity of synthetic polymers, when combined with them in nanofibrous scaffolds. Conversely, synthetic polymers can improve the electrospinnability and mechanical properties of the natural polymers. Similarly as synthetic polymers, nature-derived polymers can be more or less degradable in human tissues. Degradable polymers include collagen, gelatin, elastin, keratin, glycosaminoglycans, but also chitosan, gellan gum and PHBV, that is, polymers produced by other than mammalian organisms. Polymers produced by other organisms, such as bacteria, fungi, algae, plants or insects, are usually nondegradable in human tissues, or their degradability is limited due to lack of appropriate enzymes. These polymers include glucans, such as cellulose or dextran, and other polysaccharides and proteins, such as pullulan, alginate, pectin, and silk fibroin. Well-degradable polymers are recommended as direct scaffolds for tissue engineering, while less-degradable polymers are suitable for "intelligent" wound dressing for drug delivery and cell delivery.

Acknowledgements

This review article was supported by the Grant Agency of the Czech Republic (grants No. 17-02448S and 17-00885S).

Author details

Lucie Bacakova[1*], Julia Pajorova[1], Marketa Zikmundova[1], Elena Filova[1], Petr Mikes[2], Vera Jencova[2], Eva Kuzelova Kostakova[2] and Alla Sinica[3,4]

1 Department of Biomaterials and Tissue Engineering, Institute of Physiology of the Czech Academy of Sciences, Prague, Czech Republic

2 Faculty of Sciences, Humanities and Education, Technical University of Liberec, Liberec, Czech Republic

3 BIOCEV, 1st Faculty of Medicine, Charles University, Vestec, Czech Republic

4 Department of Analytical Chemistry, University of Chemistry and Technology Prague, Prague, Czech Republic

*Address all correspondence to: lucie.bacakova@fgu.cas.cz

References

[1] Bacakova L, Bacakova M, Pajorova J, Kudlackova R, Stankova L, Musilkova J, et al. Nanofibrous scaffolds as promising cell carriers for tissue engineering, chapter 3. In: Rahman MM, Asiri AM, editors, ISBN 978-953-51-2529-7, Print ISBN 978-953-51-2528-0, Nanofiber Research - Reaching New Heights. London, United Kingdom: IntechOpen; 2016. pp. 29-54

[2] Kim JI, Pant HR, Sim HJ, Lee KM, Kim CS. Electrospun propolis/polyurethane composite nanofibers for biomedical applications. Materials Science & Engineering. C, Materials for Biological Applications. 2014;**44**:52-57. DOI: 10.1016/j.msec.2014.07.062

[3] Drupitha MP, Bankoti K, Pal P, Das B, Parameswar R, Dhara S, et al. Morphology-induced physico-mechanical and biological characteristics of TPU-PDMS blend scaffolds for skin tissue engineering applications. Journal of Biomedical Materials Research. Part B, Applied Biomaterials. 2019;**107**(5):1634-1644. DOI: 10.1002/jbm.b.34256

[4] Arslan A, Simşek M, Aldemir SD, Kazaroğlu NM, Gümüşderelioğlu M. Honey-based PET or PET/chitosan fibrous wound dressings: Effect of honey on electrospinning process. Journal of Biomaterials Science. Polymer Edition. 2014;**25**(10):999-1012. DOI: 10.1080/09205063.2014.918455

[5] Babaeijandaghi F, Shabani I, Seyedjafari E, Naraghi ZS, Vasei M, Haddadi-Asl V, et al. Accelerated epidermal regeneration and improved dermal reconstruction achieved by polyethersulfone nanofibers. Tissue Engineering. Part A. 2010;**16**(11): 3527-3536. DOI: 10.1089/ten.TEA.2009.0829

[6] Altinbasak I, Jijie R, Barras A, Golba B, Sanyal R, Bouckaert J, et al. Reduced graphene-oxide-embedded polymeric nanofiber mats: An "on-demand" photothermally triggered antibiotic release platform. ACS Applied Materials & Interfaces. 2018;**10**(48):41098-41106. DOI: 10.1021/acsami.8b14784

[7] Zupančič Š, Sinha-Ray S, Sinha-Ray S, Kristl J, Yarin AL. Controlled release of ciprofloxacin from core-shell nanofibers with monolithic or blended core. Molecular Pharmaceutics. 2016;**13**(4):1393-1404. DOI: 10.1021/acs.molpharmaceut.6b00039

[8] Li H, Williams GR, Wu J, Lv Y, Sun X, Wu H, et al. Thermosensitive nanofibers loaded with ciprofloxacin as antibacterial wound dressing materials. International Journal of Pharmaceutics. 2017;**517**(1-2):135-147. DOI: 10.1016/j.ijpharm.2016.12.008

[9] Hejazian LB, Esmaeilzade B, Moghanni Ghoroghi F, Moradi F, Hejazian MB, Aslani A, et al. The role of biodegradable engineered nanofiber scaffolds seeded with hair follicle stem cells for tissue engineering. Iranian Biomedical Journal. 2012;**16**(4):193-201. DOI: 10.6091/ibj.1074.2012

[10] Mikes P, Horakova J, Saman A, Vejsadova L, Topham P, Punyodom W, et al. Comparison and characterization of different polyester nano/micro fibres for use in tissue engineering applications. Journal of Industrial Textiles. 2019. In press. DOI: 10.1177/1528083719848155

[11] Hoveizi E, Nabiuni M, Parivar K, Rajabi-Zeleti S, Tavakol S. Functionalisation and surface modification of electrospun polylactic acid scaffold for tissue engineering. Cell Biology International. 2014;**38**(1):41-49. DOI: 10.1002/cbin.10178

[12] Shtrichman R, Zeevi-Levin N, Zaid R, Barak E, Fishman B,

Ziskind A, et al. The generation of hybrid electrospun nanofiber layer with extracellular matrix derived from human pluripotent stem cells, for regenerative medicine applications. Tissue Engineering. Part A. 2014;**20**(19-20):2756-2767. DOI: 10.1089/ten.TEA.2013.0705

[13] Poormasjedi-Meibod MS, Salimi Elizei S, Leung V, Baradar Jalili R, Ko F, Ghahary A. Kynurenine modulates MMP-1 and type-I collagen expression via aryl hydrocarbon receptor activation in dermal fibroblasts. Journal of Cellular Physiology. 2016;**231**(12):2749-2760. DOI: 10.1002/jcp.25383

[14] Gaaz TS, Sulong AB, Akhtar MN, Kadhum AA, Mohamad AB, Al-Amiery AA. Properties and applications of polyvinyl alcohol, halloysite nanotubes and their nanocomposites. Molecules. 2015;**20**(12):22833-22847. DOI: 10.3390/molecules201219884

[15] Bacakova L, Svorcik V. Cell colonization control by physical and chemical modification of materials. In: Kimura D, editor. Cell Growth Processes: New Research. Hauppauge, New York, USA: Nova Science Publishers, Inc; 2008. pp. 5-56. ISBN 978-1-60456-123-6

[16] Bacakova L, Filova E, Parizek M, Ruml T, Svorcik V. Modulation of cell adhesion, proliferation and differentiation on materials designed for body implants. Biotechnology Advances. 2011;**29**(6):739-767. DOI: 10.1016/j.biotechadv.2011.06.004

[17] Blackstone BN, Hahn JM, McFarland KL, DeBruler DM, Supp DM, Powell HM. Inflammatory response and biomechanical properties of coaxial scaffolds for engineered skin in vitro and post-grafting. Acta Biomaterialia. 2018;**80**:247-257. DOI: 10.1016/j.actbio.2018.09.014

[18] Bačáková L, Novotná K, Sopuch T, Havelka P. Cell interaction with cellulose-based scaffolds for tissue engineering – A review. In: Mondal IH, editor. Cellulose and Cellulose Derivatives: Synthesis, Modification, Nanostructure and Applications. Hauppauge, New York, USA: Nova Science Publishers, Inc.; 2015. pp. 341-375. ISBN 978-1-63483-571-8

[19] Bacakova L, Pajorova J, Bacakova M, Skogberg A, Kallio P, Kolarova K, et al. Versatile application of nanocellulose: From industry to skin tissue engineering and wound healing. Nanomaterials. 2019;**9**(2). pii: E164. DOI: 10.3390/nano9020164

[20] Ohnkawa K. Nanofibers of cellulose and its derivatives fabricated using direct electrospinning. Molecules. 2015;**20**:9139-9154. DOI: 10.3390/molecules20059139

[21] Hu Y, Catchmark JM. Integration of cellulases into bacterial cellulose: Toward bioabsorbable cellulose composites. Journal of Biomedical Materials Research. Part B, Applied Biomaterials. 2011;**97**(1):114-123. DOI: 10.1002/jbm.b.31792

[22] Hu Y, Catchmark JM. In vitro biodegradability and mechanical properties of bioabsorbable bacterial cellulose incorporating cellulases. Acta Biomaterialia. 2011;**7**(7):2835-2845. DOI: 10.1016/j.actbio.2011.03.028

[23] Ko IK, Iwata H. An approach to constructing three-dimensional tissue. Annals of the New York Academy of Sciences. 2001;**944**:443-455. DOI: 10.1111/j.1749-6632.2001.tb03854.x

[24] Ko IK, Kato K, Iwata H. A thin carboxymethyl cellulose culture substrate for the cellulase-induced harvesting of an endothelial cell sheet. Journal of Biomaterials Science. Polymer Edition. 2005;**16**(10):1277-1291. DOI: 10.1163/156856205774269511

[25] Entcheva E, Bien H, Yin L, Chung CY, Farrell M, Kostov Y. Functional cardiac cell constructs on cellulose-based scaffolding. Biomaterials. 2004;**25**(26):5753-5762. DOI: 10.1016/j.biomaterials.2004.01.024

[26] Torres-Rendon JG, Köpf M, Gehlen D, Blaeser A, Fischer H, De Laporte L, et al. Cellulose nanofibril hydrogel tubes as sacrificial templates for freestanding tubular cell constructs. Biomacromolecules. 2016;**17**(3):905-913. DOI: 10.1021/acs.biomac.5b01593

[27] Yadav V, Paniliatis BJ, Shi H, Lee K, Cebe P, Kaplan DL. Novel in vivo-degradable cellulose-chitin copolymer from metabolically engineered Gluconacetobacter xylinus. Applied and Environmental Microbiology. 2010;**76**(18):6257-6265. DOI: 10.1128/AEM.00698-10

[28] Yadav V, Sun L, Panilaitis B, Kaplan DL. In vitro chondrogenesis with lysozyme susceptible bacterial cellulose as a scaffold. Journal of Tissue Engineering and Regenerative Medicine. 2015;**9**(12):E276-E288. DOI: 10.1002/term.1644

[29] Safaee-ArdakaniMR,Hatamian-ZarmiA, Sadat SM, Mokhtari-Hosseini ZB, Ebrahimi-Hosseinzadeh B, Rashidiani J, et al. Electrospun schizophyllan/polyvinyl alcohol blend nanofibrous scaffold as potential wound healing. International Journal of Biological Macromolecules. 2019;**127**:27-38. DOI: 10.1016/j.ijbiomac.2018.12.256

[30] Unnithan AR, Sasikala AR, Murugesan P, Gurusamy M, Wu D, Park CH, et al. Electrospun polyurethane-dextran nanofiber mats loaded with estradiol for post-menopausal wound dressing. International Journal of Biological Macromolecules. 2015;**77**:1-8. DOI: 10.1016/j.ijbiomac.2015.02.044

[31] Pan JF, Liu NH, Sun H, Xu F. Preparation and characterization of electrospun PLCL/Poloxamer nanofibers and dextran/gelatin hydrogels for skin tissue engineering. PLoS One. 2014;**9**(11):e112885. DOI: 10.1371/journal.pone.0112885

[32] Maia J, Evangelista MB, Gil H, Ferreira L. 2. Dextran-based materials for biomedical applications. In: Gil MH, editor. Carbohydrates Applications in Medicine. Kerala, India: Research Signpost; 2014. pp. 31-53. ISBN: 978-81-308-0523-8

[33] Bačáková L, Novotná K, Pařízek M. Polysaccharides as cell carriers for tissue engineering: The use of cellulose in vascular wall reconstruction. Physiological Research. 2014;**63**(Suppl 1):S29-S47

[34] Waghmare VS, Wadke PR, Dyawanapelly S, Deshpande A, Jain R, Dandekar P. Starch based nanofibrous scaffolds for wound healing applications. Bioact Mater. 2017;**3**(3):255-266. DOI: 10.1016/j.bioactmat.2017.11.006

[35] Byman E, Schultz N, Netherlands Brain Bank, Fex M, Wennström M. Brain alpha-amylase: A novel energy regulator important in Alzheimer disease? Brain Pathology. 2018;**28**(6):920-932. DOI: 10.1111/bpa.12597

[36] Abed A, Assoul N, Ba M, Derkaoui SM, Portes P, Louedec L, et al. Influence of polysaccharide composition on the biocompatibility of pullulan/dextran-based hydrogels. Journal of Biomedical Materials Research. Part A. 2011;**96**(3):535-542. DOI: 10.1002/jbm.a.33007

[37] Xu F, Weng B, Gilkerson R, Materon LA, Lozano K. Development of tannic acid/chitosan/pullulan composite nanofibers from aqueous solution for potential applications as wound dressing. Carbohydrate Polymers.

2015;**115**:16-24. DOI: 10.1016/j.carbpol.2014.08.081

[38] Shi L, Le Visage C, Chew SY. Long-term stabilization of polysaccharide electrospun fibres by in situ cross-linking. Journal of Biomaterials Science. Polymer Edition. 2011;**22**(11):1459-1472. DOI: 10.1163/092050610X512108

[39] Krishnan R, Rajeswari R, Venugopal J, Sundarrajan S, Sridhar R, Shayanti M, et al. Polysaccharide nanofibrous scaffolds as a model for in vitro skin tissue regeneration. Journal of Materials Science. Materials in Medicine. 2012;**23**(6):1511-1519. DOI: 10.1007/s10856-012-4630-6

[40] Liu X, Chang M, He B, Meng L, Wang X, Sun R, et al. A one-pot strategy for preparation of high-strength carboxymethyl xylan-g-poly(acrylic acid) hydrogels with shape memory property. Journal of Colloid and Interface Science. 2019;**538**:507-518. DOI: 10.1016/j.jcis.2018.12.023

[41] Sobhanian P, Khorram M, Hashemi SS, Mohammadi A. Development of nanofibrous collagen-grafted poly (vinyl alcohol)/gelatin/alginate scaffolds as potential skin substitute. International Journal of Biological Macromolecules. 2019;**130**:977-987. DOI: 10.1016/j.ijbiomac.2019.03.045

[42] Coşkun G, Karaca E, Ozyurtlu M, Ozbek S, Yermezler A, Cavuşoğlu I. Histological evaluation of wound healing performance of electrospun poly(vinyl alcohol)/sodium alginate as wound dressing in vivo. Bio-medical Materials and Engineering. 2014;**24**(2):1527-1536. DOI: 10.3233/BME-130956

[43] Jeong SI, Krebs MD, Bonino CA, Khan SA, Alsberg E. Electrospun alginate nanofibers with controlled cell adhesion for tissue engineering. Macromolecular Bioscience. 2010;**10**(8):934-943. DOI: 10.1002/mabi.201000046

[44] Tort S, Acartürk F, Beşikci A. Evaluation of three-layered doxycycline-collagen loaded nanofiber wound dressing. International Journal of Pharmaceutics. 2017;**529**(1-2):642-653. DOI: 10.1016/j.ijpharm.2017.07.027

[45] Byeon SY, Cho MK, Shim KH, Kim HJ, Song HG, Shin HS. Development of a Spirulina extract/alginate-imbedded PCL nanofibrous cosmetic patch. Journal of Microbiology and Biotechnology. 2017;**27**(9):1657-1663. DOI: 10.4014/jmb.1701.01025

[46] Hoseinpour Najar M, Minaiyan M. Taheri A. Preparation and in vivo evaluation of a novel gel-based wound dressing using arginine-alginate surface-modified chitosan nanofibers. Journal of Biomaterials Applications. 2018;**32**(6):689-701. DOI: 10.1177/0885328217739562

[47] Hu WP, Zhang B, Zhang J, Luo WL, Guo Y, Chen SJ, et al. Ag/alginate nanofiber membrane for flexible electronic skin. Nanotechnology. 2017;**28**(44):445502. DOI: 10.1088/1361-6528/aa8746

[48] Guarino V, Caputo T, Altobelli R, Ambrosio L. Degradation properties and metabolic activity of alginate and chitosan polyelectrolytes for drug delivery and tissue engineering applications. AIMS Materials Science. 2015;**2**(4):497-502. DOI: 10.3934/matersci.2015.4.497

[49] Voragen AGJ, Coenen G-J, Verhoef RP, Schols HA. Pectin, a versatile polysaccharide present in plant cell walls. Structural Chemistry. 2009;**20**:263-275. DOI: 10.1007/s11224-009-9442-z

[50] Archana D, Dutta J, Dutta PK. Evaluation of chitosan nano dressing

for wound healing: Characterization, in vitro and in vivo studies. International Journal of Biological Macromolecules. 2013;**57**:193-203. DOI: 10.1016/j.ijbiomac.2013.03.002

[51] Tayi L, Maku RV, Patel HK, Sonti RV. Identification of pectin degrading enzymes secreted by Xanthomonas oryzae pv. oryzae and determination of their role in virulence on rice. PLoS One. 2016;**11**(12):e0166396. DOI: 10.1371/journal.pone.0166396

[52] Martos MA, Zubreski ER, Garro OA, Hours RA. Production of pectinolytic enzymes by the yeast Wickerhanomyces anomalus isolated from citrus fruits peels. Biotechnology Research International. 2013;**2013**:435154. DOI: 10.1155/2013/435154

[53] Huber DJ, Karakurt Y, Jeong J, et al. Pectin degradation in ripening and wounded fruits. The Revista Brasileira de Fisiologia Vegetal (Brazilian Journal of Plant Physiology). 2001;**13**(2):224-241. DOI: 10.1590/S0103-31312001000200009

[54] Lin HY, Chen HH, Chang SH, Ni TS. Pectin-chitosan-PVA nanofibrous scaffold made by electrospinning and its potential use as a skin tissue scaffold. Journal of Biomaterials Science. Polymer Edition. 2013;**24**(4):470-484. DOI: 10.1080/09205063.2012.693047

[55] Lin HY, Chen SH, Chang SH, Huang ST. Tri-layered chitosan scaffold as a potential skin substitute. Journal of Biomaterials Science. Polymer Edition. 2015;**26**(13):855-867. DOI: 10.1080/09205063.2015.1061350

[56] Chen S, Cui S, Zhang H, Pei X, Hu J, Zhou Y, et al. Cross-linked pectin nanofibers with enhanced cell adhesion. Biomacromolecules. 2018;**19**(2):490-498. DOI: 10.1021/acs.biomac.7b01605

[57] Saruchi, Kaith BS, Jindal R, Kumar V. Biodegradation of gum tragacanth acrylic acid based hydrogel and its impact on soil fertility. Polymer Degradation and Stability. 2015;**115**:24-31. DOI: 10.1016/j.polymdegradstab.2015.02.009

[58] Hindi SSZ, Albureikan MO, Al-Ghamdi AA, Alhummiany H, Ansari MS. Synthesis, characterization and biodegradation of gum arabic-based bioplastic membranes. Nanoscience and Nanotechnology Research. 2017;**4**(2):32-42. DOI: 10.12691/nnr-4-2-1

[59] Zarekhalili Z, Bahrami SH, Ranjbar-Mohammadi M, Milan PB. Fabrication and characterization of PVA/gum tragacanth/PCL hybrid nanofibrous scaffolds for skin substitutes. International Journal of Biological Macromolecules. 2017;**94**(Pt A):679-690. DOI: 10.1016/j.ijbiomac.2016.10.042

[60] Ranjbar-Mohammadi M, Rabbani S, Bahrami SH, Joghataei MT, Moayer F. Antibacterial performance and in vivo diabetic wound healing of curcumin loaded gum tragacanth/poly(ε-caprolactone) electrospun nanofibers. Materials Science & Engineering. C, Materials for Biological Applications. 2016;**69**:1183-1191. DOI: 10.1016/j.msec.2016.08.032

[61] Pedram Rad Z, Mokhtari J, Abbasi M. Calendula officinalis extract/PCL/Zein/gum arabic nanofibrous bio-composite scaffolds via suspension, two-nozzle and multilayer electrospinning for skin tissue engineering. International Journal of Biological Macromolecules. 2019;**135**:530-543. DOI: 10.1016/j.ijbiomac.2019.05.204

[62] Srivastava CM, Purwar R. Fabrication of robust Antheraea assama fibroin nanofibrous mat using ionic liquid for skin tissue engineering.

Materials Science & Engineering. C, Materials for Biological Applications. 2016;**68**:276-290. DOI: 10.1016/j.msec.2016.05.020

[63] Srivastava CM, Purwar R, Gupta AP. Enhanced potential of biomimetic, silver nanoparticles functionalized Antheraea mylitta (tasar) silk fibroin nanofibrous mats for skin tissue engineering. International Journal of Biological Macromolecules. 2019;**130**:437-453. DOI: 10.1016/j.ijbiomac.2018.12.255

[64] Chouhan D, Chakraborty B, Nandi SK, Mandal BB. Role of non-mulberry silk fibroin in deposition and regulation of extracellular matrix towards accelerated wound healing. Acta Biomaterialia. 2017;**48**:157-174. DOI: 10.1016/j.actbio.2016.10.019

[65] Cao Y, Wang B. Biodegradation of silk biomaterials. International Journal of Molecular Sciences. 2009;**10**(4):1514-1524. DOI: 10.3390/ijms10041514

[66] Wang Y, Rudym DD, Walsh A, Abrahamsen L, Kim HJ, Kim HS, et al. In vivo degradation of three-dimensional silk fibroin scaffolds. Biomaterials. 2008;**29**(24-25):3415-3428. DOI: 10.1016/j.biomaterials.2008.05.002

[67] Lee JM, Chae T, Sheikh FA, Ju HW, Moon BM, Park HJ, et al. Three dimensional poly(ε-caprolactone) and silk fibroin nanocomposite fibrous matrix for artificial dermis. Materials Science & Engineering. C, Materials for Biological Applications. 2016;**68**:758-767. DOI: 10.1016/j.msec.2016.06.019

[68] Sridhar S, Venugopal JR, Ramakrishna S. Improved regeneration potential of fibroblasts using ascorbic acid-blended nanofibrous scaffolds. Journal of Biomedical Materials Research. Part A. 2015;**103**(11):3431-3440. DOI: 10.1002/jbm.a.35486

[69] Zhou Y, Yang H, Liu X, Mao J, Gu S, Xu W. Electrospinning of carboxyethyl chitosan/poly(vinyl alcohol)/silk fibroin nanoparticles for wound dressings. International Journal of Biological Macromolecules. 2013;**53**:88-92. DOI: 10.1016/j.ijbiomac.2012.11.013

[70] Yoo CR, Yeo IS, Park KE, Park JH, Lee SJ, Park WH, et al. Effect of chitin/silk fibroin nanofibrous bicomponent structures on interaction with human epidermal keratinocytes. International Journal of Biological Macromolecules. 2008;**42**(4):324-334. DOI: 10.1016/j.ijbiomac.2007.12.004

[71] Shefa AA, Amirian J, Kang HJ, Bae SH, Jung HI, Choi HJ, et al. In vitro and in vivo evaluation of effectiveness of a novel TEMPO-oxidized cellulose nanofiber-silk fibroin scaffold in wound healing. Carbohydrate Polymers. 2017;**177**:284-296. DOI: 10.1016/j.carbpol.2017.08.130

[72] Xin S, Li X, Wang Q, Huang R, Xu X, Lei Z, et al. Novel layer-by-layer structured nanofibrous mats coated by protein films for dermal regeneration. Journal of Biomedical Nanotechnology. 2014;**10**(5):803-810. DOI: 10.1166/jbn.2014.1748

[73] Yeo IS, Oh JE, Jeong L, Lee TS, Lee SJ, Park WH, et al. Collagen-based biomimetic nanofibrous scaffolds: Preparation and characterization of collagen/silk fibroin bicomponent nanofibrous structures. Biomacromolecules. 2008;**9**(4):1106-1116. DOI: 10.1021/bm700875a

[74] Shan YH, Peng LH, Liu X, Chen X, Xiong J, Gao JQ. Silk fibroin/gelatin electrospun nanofibrous dressing functionalized with astragaloside IV induces healing and anti-scar effects on burn wound. International Journal of Pharmaceutics. 2015;**479**(2):291-301. DOI: 10.1016/j.ijpharm.2014.12.067

[75] Li L, Qian Y, Jiang C, Lv Y, Liu W, Zhong L, et al. The use of hyaluronan

to regulate protein adsorption and cell infiltration in nanofibrous scaffolds. Biomaterials. 2012;**33**(12):3428-3445. DOI: 10.1016/j.biomaterials.2012.01.038

[76] Sheng X, Fan L, He C, Zhang K, Mo X, Wang H. Vitamin E-loaded silk fibroin nanofibrous mats fabricated by green process for skin care application. International Journal of Biological Macromolecules. 2013;**56**:49-56. DOI: 10.1016/j.ijbiomac.2013.01.029

[77] Fan L, Cai Z, Zhang K, Han F, Li J, He C, et al. Green electrospun pantothenic acid/silk fibroin composite nanofibers: Fabrication, characterization and biological activity. Colloids and Surfaces. B, Biointerfaces. 2014;**117**:14-20. DOI: 10.1016/j.colsurfb.2013.12.030

[78] Lin S, Chen M, Jiang H, Fan L, Sun B, Yu F, et al. Green electrospun grape seed extract-loaded silk fibroin nanofibrous mats with excellent cytocompatibility and antioxidant effect. Colloids and Surfaces. B, Biointerfaces. 2016;**139**:156-163. DOI: 10.1016/j.colsurfb.2015.12.001

[79] Kandhasamy S, Arthi N, Arun RP, Verma RS. Synthesis and fabrication of novel quinone-based chromenopyrazole antioxidant-laden silk fibroin nanofibers scaffold for tissue engineering applications. Materials Science & Engineering. C, Materials for Biological Applications. 2019;**102**:773-787. DOI: 10.1016/j.msec.2019.04.076

[80] Suganya S, Venugopal J, Ramakrishna S, Lakshmi BS, Dev VR. Naturally derived biofunctional nanofibrous scaffold for skin tissue regeneration. International Journal of Biological Macromolecules. 2014;**68**:135-143. DOI: 10.1016/j.ijbiomac.2014.04.031

[81] Lee OJ, Ju HW, Kim JH, Lee JM, Ki CS, Kim JH, et al. Development of artificial dermis using 3D electrospun silk fibroin nanofiber matrix. Journal of Biomedical Nanotechnology. 2014;**10**(7):1294-1303

[82] Park YR, Ju HW, Lee JM, Kim DK, Lee OJ, Moon BM, et al. Three-dimensional electrospun silk-fibroin nanofiber for skin tissue engineering. International Journal of Biological Macromolecules. 2016;**93**(Pt B):1567-1574. DOI: 10.1016/j.ijbiomac.2016.07.047

[83] Gholipourmalekabadi M, Samadikuchaksaraei A, Seifalian AM, Urbanska AM, Ghanbarian H, Hardy JG, et al. Silk fibroin/amniotic membrane 3D bi-layered artificial skin. Biomedical Materials. 2018;**13**(3):035003. DOI: 10.1088/1748-605X/aa999b

[84] Xie SY, Peng LH, Shan YH, Niu J, Xiong J, Gao JQ. Adult stem cells seeded on electrospinning silk fibroin nanofiberous scaffold enhance wound repair and regeneration. Journal of Nanoscience and Nanotechnology. 2016;**16**(6):5498-5505. DOI: 10.1166/jnn.2016.11730

[85] Sapru S, Das S, Mandal M, Ghosh AK, Kundu SC. Prospects of nonmulberry silk protein sericin-based nanofibrous matrices for wound healing - In vitro and in vivo investigations. Acta Biomaterialia. 2018;**78**:137-150. DOI: 10.1016/j.actbio.2018.07.047

[86] Bhowmick S, Scharnweber D, Koul V. Co-cultivation of keratinocyte-human mesenchymal stem cell (hMSC) on sericin loaded electrospun nanofibrous composite scaffold (cationic gelatin/hyaluronan/chondroitin sulfate) stimulates epithelial differentiation in hMSCs: In vitro study. Biomaterials. 2016;**88**:83-96. DOI: 10.1016/j.biomaterials.2016.02.034

[87] Gilotra S, Chouhan D, Bhardwaj N, Nandi SK, Mandal BB. Potential of silk sericin based nanofibrous mats

for wound dressing applications. Materials Science & Engineering. C, Materials for Biological Applications. 2018;**90**:420-432. DOI: 10.1016/j.msec.2018.04.077

[88] Zhao R, Li X, Sun B, Zhang Y, Zhang D, Tang Z, et al. Electrospun chitosan/sericin composite nanofibers with antibacterial property as potential wound dressings. International Journal of Biological Macromolecules. 2014;**68**:92-97. DOI: 10.1016/j.ijbiomac.2014.04.029

[89] Law JX, Liau LL, Saim A, Yang Y, Idrus R. Electrospun collagen nanofibers and their applications in skin tissue engineering. Tissue Eng Regen Med. 2017;**14**(6):699-718. DOI: 10.1007/s13770-017-0075-9

[90] Wang Y, Zhang CL, Zhang Q, Li P. Composite electrospun nanomembranes of fish scale collagen peptides/chito-oligosaccharides: Antibacterial properties and potential for wound dressing. International Journal of Nanomedicine. 2011;**6**: 667-676. DOI: 10.2147/IJN.S17547

[91] Zhou T, Wang N, Xue Y, Ding T, Liu X, Mo X, et al. Electrospun tilapia collagen nanofibers accelerating wound healing via inducing keratinocytes proliferation and differentiation. Colloids and Surfaces. B, Biointerfaces. 2016;**143**:415-422. DOI: 10.1016/j.colsurfb.2016.03.052

[92] Le Corre-Bordes D, Hofman K, Hall B. Guide to electrospinning denatured whole chain collagen from hoki fish using benign solvents. International Journal of Biological Macromolecules. 2018;**112**:1289-1299. DOI: 10.1016/j.ijbiomac.2018.02.088

[93] Zhou T, Sui B, Mo X, Sun J. Multifunctional and biomimetic fish collagen/bioactive glass nanofibers: Fabrication, antibacterial activity and inducing skin regeneration in vitro and in vivo. International Journal of Nanomedicine. 2017;**12**:3495-3507. DOI: 10.2147/IJN.S132459

[94] Chen J, Gao K, Liu S, Wang S, Elango J, Bao B, et al. Fish collagen surgical compress repairing characteristics on wound healing process In vivo. Marine Drugs. 2019;**17**. pii: E33. DOI: 10.3390/md17010033

[95] Cumming MH, Leonard AR, LeCorre-Bordes DS, Hofman K. Intra-fibrillar citric acid crosslinking of marine collagen electrospun nanofibres. International Journal of Biological Macromolecules. 2018;**114**:874-881. DOI: 10.1016/j.ijbiomac.2018.03.180

[96] Ramanathan G, Muthukumar T, Sivagnanam T. In vivo efficiency of the collagen coated nanofibrous scaffold and their effect on growth factors and pro-inflammatory cytokines in wound healing. European Journal of Pharmacology. 2017;**814**:45-55. DOI: 10.1016/j.ejphar.2017.08.003

[97] Dhand C, Balakrishnan Y, Ong ST, Dwivedi N, Venugopal JR, Harini S, et al. Antimicrobial quaternary ammonium organosilane cross-linked nanofibrous collagen scaffolds for tissue engineering. International Journal of Nanomedicine. 2018;**13**:4473-4492. DOI: 10.2147/IJN.S159770

[98] Ravichandran R, Venugopal JR, Sundarrajan S, Mukherjee S, Sridhar R, Ramakrishna S. Composite poly-L-lactic acid/poly-(α,β)-DL-aspartic acid/collagen nanofibrous scaffolds for dermal tissue regeneration. Materials Science & Engineering. C, Materials for Biological Applications. 2012;**32**(6):1443-1451. DOI: 10.1016/j.msec.2012.04.024

[99] Alamein MA, Stephens S, Liu Q, Skabo S, Warnke PH. Mass production of nanofibrous extracellular matrix with controlled 3D morphology for

large-scale soft tissue regeneration. Tissue Engineering. Part C, Methods. 2013;**19**(6):458-472. DOI: 10.1089/ten.TEC.2012.0417

[100] Peh P, Lim NS, Blocki A, Chee SM, Park HC, Liao S, et al. Simultaneous delivery of highly diverse bioactive compounds from blend electrospun fibers for skin wound healing. Bioconjugate Chemistry. 2015;**26**(7):1348-1358. DOI: 10.1021/acs.bioconjchem.5b00123

[101] Gümüşderelioğlu M, Dalkıranoğlu S, Aydın RS, Cakmak S. A novel dermal substitute based on biofunctionalized electrospun PCL nanofibrous matrix. Journal of Biomedical Materials Research. Part A. 2011;**98**(3):461-472. DOI: 10.1002/jbm.a.33143

[102] Albright V, Xu M, Palanisamy A, Cheng J, Stack M, Zhang B, et al. Micelle-coated, hierarchically structured nanofibers with dual-release capability for accelerated wound healing and infection control. Advanced Healthcare Materials. 2018;**7**(11):e1800132. DOI: 10.1002/adhm.201800132

[103] Abdul Khodir WKW, Abdul Razak AH, Ng MH, Guarino V, Susanti D. Encapsulation and characterization of gentamicin sulfate in the collagen added electrospun nanofibers for skin regeneration. J Funct Biomater. 2018;**9**(2):E36. DOI: 10.3390/jfb9020036

[104] Wang C, Wang Q, Gao W, Zhang Z, Lou Y, Jin H, et al. Highly efficient local delivery of endothelial progenitor cells significantly potentiates angiogenesis and full-thickness wound healing. Acta Biomaterialia. 2018;**69**:156-169. DOI: 10.1016/j.actbio.2018.01.019

[105] Ghosal K, Manakhov A, Zajíčková L, Thomas S. Structural and surface compatibility study of modified electrospun poly(ε-caprolactone) (PCL) composites for skin tissue engineering. AAPS PharmSciTech. 2017;**18**(1):72-81. DOI: 10.1208/s12249-016-0500-8

[106] Xie X, Li D, Su C, Cong W, Mo X, Hou G, et al. Functionalized biomimetic composite nanfibrous scaffolds with antibacterial and hemostatic efficacy for facilitating wound healing. Journal of Biomedical Nanotechnology. 2019;**15**(6):1267-1279. DOI: 10.1166/jbn.2019.2756

[107] Yao CH, Chen KY, Chen YS, Li SJ, Huang CH. Lithospermi radix extract-containing bilayer nanofiber scaffold for promoting wound healing in a rat model. Materials Science & Engineering. C, Materials for Biological Applications. 2019;**96**:850-858. DOI: 10.1016/j.msec.2018.11.053

[108] Aldana AA, Abraham GA. Current advances in electrospun gelatin-based scaffolds for tissue engineering applications. International Journal of Pharmaceutics. 2017;**523**(2):441-453. DOI: 10.1016/j.ijpharm.2016.09.044

[109] Yao CH, Lee CY, Huang CH, Chen YS, Chen KY. Novel bilayer wound dressing based on electrospun gelatin/keratin nanofibrous mats for skin wound repair. Materials Science & Engineering. C, Materials for Biological Applications. 2017;**79**:533-540. DOI: 10.1016/j.msec.2017.05.076

[110] Adeli-Sardou M, Yaghoobi MM, Torkzadeh-Mahani M, Dodel M. Controlled release of lawsone from polycaprolactone/gelatin electrospun nano fibers for skin tissue regeneration. International Journal of Biological Macromolecules. 2019;**124**:478-491. DOI: 10.1016/j.ijbiomac.2018.11.237

[111] Baghersad S, Hajir Bahrami S, Mohammadi MR, Mojtahedi MRM, Milan PB. Development of biodegradable electrospun gelatin/aloe-vera/poly (ε-caprolactone) hybrid nanofibrous

scaffold for application as skin substitutes. Materials Science & Engineering. C, Materials for Biological Applications. 2018;**93**:367-379. DOI: 10.1016/j.msec.2018.08.020

[112] Dias JR, Baptista-Silva S, Sousa A, Oliveira AL, Bártolo PJ, Granja PL. Biomechanical performance of hybrid electrospun structures for skin regeneration. Materials Science & Engineering. C, Materials for Biological Applications. 2018;**93**:816-827. DOI: 10.1016/j.msec.2018.08.050

[113] Chandrasekaran AR, Venugopal J, SundarrajanS,RamakrishnaS.Fabrication of a nanofibrous scaffold with improved bioactivity for culture of human dermal fibroblasts for skin regeneration. Biomedical Materials. 2011;**6**(1):015001. DOI: 10.1088/1748-6041/6/1/015001

[114] Jin G, Prabhakaran MP, Kai D, Ramakrishna S. Controlled release of multiple epidermal induction factors through core-shell nanofibers for skin regeneration. European Journal of Pharmaceutics and Biopharmaceutics. 2013;**85**(3 Pt A):689-698. DOI: 10.1016/j.ejpb.2013.06.002

[115] Mao W, Kang MK, Shin JU, Son YJ, Kim HS, Yoo HS. Coaxial hydro-nanofibrils for self-assembly of cell sheets producing skin bilayers. ACS Applied Materials & Interfaces. 2018;**10**(50):43503-43511. DOI: 10.1021/acsami.8b17740

[116] Kim JW, Kim MJ, Ki CS, Kim HJ, Park YH. Fabrication of bi-layer scaffold of keratin nanofiber and gelatin-methacrylate hydrogel: Implications for skin graft. International Journal of Biological Macromolecules. 2017;**105**(Pt 1):541-548. DOI: 10.1016/j.ijbiomac.2017.07.067

[117] Zhao X, Sun X, Yildirimer L, Lang Q, Lin ZYW, Zheng R, et al. Cell infiltrative hydrogel fibrous scaffolds for accelerated wound healing. Acta Biomaterialia. 2017;**49**:66-77. DOI: 10.1016/j.actbio.2016.11.017

[118] DeFrates KG, Moore R, Borgesi J, Lin G, Mulderig T, Beachley V, et al. Protein-based fiber materials in medicine: A review. Nanomaterials. 2018;**8**(7). pii: E457. DOI: 10.3390/nano8070457

[119] Khalili S, Khorasani SN, Razavi SM, Hashemibeni B, Tamayol A. Nanofibrous scaffolds with biomimetic composition for skin regeneration. Applied Biochemistry and Biotechnology. 2019;**187**(4):1193-1203. DOI: 10.1007/s12010-018-2871-7

[120] Riedel T, Brynda E, Dyr JE, Houska M. Controlled preparation of thin fibrin films immobilized at solid surfaces. Journal of Biomedical Materials Research. Part A. 2009;**88**(2):437-447. DOI: 10.1002/jbm.a.31755

[121] Law JX, Musa F, Ruszymah BH, El Haj AJ, Yang Y. A comparative study of skin cell activities in collagen and fibrin constructs. Medical Engineering & Physics. 2016;**38**(9):854-861. DOI: 10.1016/j.medengphy.2016.05.017

[122] Pajorova J, Bacakova M, Musilkova J, Broz A, Hadraba D, Lopot F, et al. Morphology of a fibrin nanocoating influences dermal fibroblast behavior. International Journal of Nanomedicine. 2018;**13**:3367-3380. DOI: 10.2147/IJN.S162644

[123] Bacakova M, Pajorova J, Broz A, Hadraba D, Lopot F, Zavadakova A, et al. A two-layer skin construct consisting of a collagen hydrogel reinforced by a fibrin-coated polylactide nanofibrous membrane. International Journal of Nanomedicine. 2019;**14**:5033-5050. DOI: 10.2147/IJN.S200782

[124] Mirzaei-Parsa MJ, Ghanbari H, Alipoor B, Tavakoli A, Najafabadi MRH, Faridi-Majidi R. Nanofiber-acellular

dermal matrix as a bilayer scaffold containing mesenchymal stem cell for healing of full-thickness skin wounds. Cell and Tissue Research. 2019;**375**(3):709-721. DOI: 10.1007/s00441-018-2927-6

[125] Wang J, Hao S, Luo T, Zhou T, Yang X, Wang B. Keratose/poly (vinyl alcohol) blended nanofibers: Fabrication and biocompatibility assessment. Materials Science & Engineering. C, Materials for Biological Applications. 2017;**72**:212-219. DOI: 10.1016/j.msec.2016.11.071

[126] Giuri D, Barbalinardo M, Sotgiu G, Zamboni R, Nocchetti M, Donnadio A, et al. Nano-hybrid electrospun non-woven mats made of wool keratin and hydrotalcites as potential bio-active wound dressings. Nanoscale. 2019;**11**(13):6422-6430. DOI: 10.1039/c8nr10114k

[127] Cruz-Maya I, Guarino V, Almaguer-Flores A, Alvarez-Perez MA, Varesano A, Vineis C. Highly polydisperse keratin rich nanofibers: Scaffold design and in vitro characterization. Journal of Biomedical Materials Research. Part A. 2019;**107**(8):1803-1813. DOI: 10.1002/jbm.a.36699

[128] Zahedi E, Esmaeili A, Eslahi N, Shokrgozar MA, Simchi A. Fabrication and characterization of core-shell electrospun fibrous mats containing medicinal herbs for wound healing and skin tissue engineering. Marine Drugs. 2019;**17**(1). pii: E27. DOI: 10.3390/md17010027

[129] Yan S, Zhang Q, Wang J, Liu Y, Lu S, Li M, et al. Silk fibroin/chondroitin sulfate/hyaluronic acid ternary scaffolds for dermal tissue reconstruction. Acta Biomaterialia. 2013;**9**(6):6771-6782. DOI: 10.1016/j.actbio.2013.02.016

[130] Li J, He A, Han CC, Fang D, Hsiao BS, Chu B. Electrospinning of hyaluronic acid (HA) and HA/gelatin blends. Macromolecular Rapid Communications. 2006;**27**:114-120. DOI: 10.1002/marc.200500726

[131] Séon-Lutz M, Couffin A-C, Vignoud S, Schlatter G, Hébraud A. Electrospinning in water and in situ crosslinking of hyaluronic acid / cyclodextrin nanofibers: Towards wound dressing with controlled drug release. Carbohydrate Polymers. 2019;**207**:276-287. DOI: 10.1016/j.carbpol.2018.11.085

[132] Um IC, Fang D, Hsiao BS, Okamoto A, Chu B. Electro-spinning and electro-blowing of hyaluronic acid. Biomacromolecules. 2004;**5**(4):1428-1436. DOI: 10.1021/bm034539b

[133] Pokorny M, Rassushin V, Wolfova L, Velebny V. Increased production of nanofibrous materials by electroblowing from blends of hyaluronic acid and polyethylene oxide. Polymer Engineering and Science. 2016;**56**:932-938. DOI: 10.1002/pen.24322

[134] Qian Y, Li L, Jiang C, Xu W, Lv Y, Zhong L, et al. The effect of hyaluronan on the motility of skin dermal fibroblasts in nanofibrous scaffolds. International Journal of Biological Macromolecules. 2015;**79**:133-143. DOI: 10.1016/j.ijbiomac.2015.04.059

[135] Stodolak-Zych E, Rozmus K, Dzierzkowska E, Zych Ł, Rapacz-Kmita A, Gargas M, et al. The membrane with polylactide and hyaluronic fibers for skin substitute. Acta of Bioengineering and Biomechanics. 2018;**20**(4):91-99. DOI: 10.5277/ABB-01199-2018-02

[136] Kurpinski KT, Stephenson JT, Janairo RR, Lee H, Li S. The effect of fiber alignment and heparin coating on cell infiltration into nanofibrous PLLA scaffolds. Biomaterials. 2010;**31**(13):3536-3542. DOI: 10.1016/j.biomaterials.2010.01.062

[137] Yergoz F, Hastar N, Cimenci CE, Ozkan AD, Tekinay T, Guler MO, et al. Heparin mimetic peptide nanofiber gel promotes regeneration of full thickness burn injury. Biomaterials. 2017;**134**:117-127. DOI: 10.1016/j.biomaterials.2017.04.040

[138] Sadeghi A, Zandi M, Pezeshki-Modaress M, Rajabi S. Tough, hybrid chondroitin sulfate nanofibers as a promising scaffold for skin tissue engineering. International Journal of Biological Macromolecules. 2019;**132**: 63-75. DOI: 10.1016/j.ijbiomac.2019.03.208. 27

[139] Pezeshki-Modaress M, Mirzadeh H, Zandi M, Rajabi-Zeleti S, Sodeifi N, Aghdami N, et al. Gelatin/chondroitin sulfate nanofibrous scaffolds for stimulation of wound healing: In-vitro and in-vivo study. Journal of Biomedical Materials Research. Part A. 2017;**105**(7):2020-2034. DOI: 10.1002/jbm.a.35890

[140] Azuma K, Ifuku S, Osaki T, Okamoto Y, Minami S. Preparation and biomedical applications of chitin and chitosan nanofibers. Journal of Biomedical Nanotechnology. 2014;**10**(10):2891-2920. DOI: 10.1166/jbn.2014.1882

[141] Kai D, Liow SS, Loh XJ. Biodegradable polymers for electrospinning: towards biomedical applications. Materials Science and Engineering C: Materials for Biological Applications. 2014;**45**:659-670. DOI: 10.1016/j.msec.2014.04.051

[142] Pal P, Dadhich P, Srivas PK, Das B, Maulik D, Dhara S. Bilayered nanofibrous 3D hierarchy as skin rudiment by emulsion electrospinning for burn wound management. Biomaterials Science. 2017;**5**(9): 1786-1799. DOI: 10.1039/c7bm00174f

[143] Gomes S, Rodrigues G, Martins G, Henriques C, Silva JC. Evaluation of nanofibrous scaffolds obtained from blends of chitosan, gelatin and polycaprolactone for skin tissue engineering. International Journal of Biological Macromolecules. 2017;**102**:1174-1185. DOI: 10.1016/j.ijbiomac.2017.05.004

[144] Mahdavi M, Mahmoudi N, Rezaie Anaran F, Simchi A. Electrospinning of nanodiamond-modified polysaccharide nanofibers with physico-mechanical properties close to natural skins. Marine Drugs. 2016;**14**(7). pii: E128. DOI: 10.3390/md14070128

[145] Veleirinho B, Coelho DS, Dias PF, Maraschin M, Ribeiro-do-Valle RM, Lopes-da-Silva JA. Nanofibrous poly(3-hydroxybutyrate-co-3-hydroxyvalerate)/chitosan scaffolds for skin regeneration. International Journal of Biological Macromolecules. 2012;**51**(4):343-350. DOI: 10.1016/j.ijbiomac.2012.05.023

[146] Shalumon KT, Sathish D, Nair SV, Chennazhi KP, Tamura H, Jayakumar R. Fabrication of aligned poly(lactic acid)-chitosan nanofibers by novel parallel blade collector method for skin tissue engineering. Journal of Biomedical Nanotechnology. 2012;**8**(3):405-416. DOI: 10.1166/jbn.2012.1395

[147] Mo Y, Guo R, Zhang Y, Xue W, Cheng B, Zhang Y. Controlled dual delivery of angiogenin and curcumin by electrospun nanofibers for skin regeneration. Tissue Engineering. Part A. 2017;**23**(13-14):597-608. DOI: 10.1089/ten.tea.2016.0268

[148] Mengistu Lemma S, Bossard F, Rinaudo M. Preparation of pure and stable chitosan nanofibers by electrospinning in the presence of poly(ethylene oxide). International Journal of Molecular Sciences. 2016;**17**(11):E1790. DOI: 10.3390/ijms17111790

[149] Koosha M, Raoufi M, Moravvej H. One-pot reactive

electrospinning of chitosan/PVA hydrogel nanofibers reinforced by halloysite nanotubes with enhanced fibroblast cell attachment for skin tissue regeneration. Colloids and Surfaces. B, Biointerfaces. 2019;**179**:270-279. DOI: 10.1016/j.colsurfb.2019.03.054

[150] Mahmoudi N, Eslahi N, Mehdipour A, Mohammadi M, Akbari M, Samadikuchaksaraei A, et al. Temporary skin grafts based on hybrid graphene oxide-natural biopolymer nanofibers as effective wound healing substitutes: Pre-clinical and pathological studies in animal models. Journal of Materials Science. Materials in Medicine. 2017;**28**(5):73. DOI: 10.1007/s10856-017-5874-y

[151] Yousefi I, Pakravan M, Rahimi H, Bahador A, Farshadzadeh Z, Haririan I. An investigation of electrospun henna leaves extract-loaded chitosan based nanofibrous mats for skin tissue engineering. Materials Science & Engineering. C, Materials for Biological Applications. 2017;**75**:433-444. DOI: 10.1016/j.msec.2017.02.076

[152] Piran M, Vakilian S, Piran M, Mohammadi-Sangcheshmeh A, Hosseinzadeh S, Ardeshirylajimi A. In vitro fibroblast migration by sustained release of PDGF-BB loaded in chitosan nanoparticles incorporated in electrospun nanofibers for wound dressing applications. Artif Cells Nanomed Biotechnol. 2018;**46**(supp 1):511-520. DOI: 10.1080/21691401.2018.1430698

[153] Tanha S, Rafiee-Tehrani M, Abdollahi M, Vakilian S, Esmaili Z, Naraghi ZS, et al. G-CSF loaded nanofiber/nanoparticle composite coated with collagen promotes wound healing in vivo. Journal of Biomedical Materials Research. Part A. 2017;**105**(10): 2830-2842. DOI: 10.1002/jbm.a.36135

[154] Noh HK, Lee SW, Kim JM, Oh JE, Kim KH, Chung CP, et al. Electrospinning of chitin nanofibers: Degradation behavior and cellular response to normal human keratinocytes and fibroblasts. Biomaterials. 2006;**27**(21):3934-3944. DOI: 10.1016/j.biomaterials.2006.03.016

[155] Vashisth P, Pruthi V. Synthesis and characterization of crosslinked gellan/PVA nanofibers for tissue engineering application. Materials Science & Engineering. C, Materials for Biological Applications. 2016;**67**:304-312. DOI: 10.1016/j.msec.2016.05.049

[156] Vashisth P, Nikhil K, Roy P, Pruthi PA, Singh RP, Pruthi V. A novel gellan-PVA nanofibrous scaffold for skin tissue regeneration: Fabrication and characterization. Carbohydrate Polymers. 2016;**136**:851-859. DOI: 10.1016/j.carbpol.2015.09.113

[157] Vashisth P, Srivastava AK, Nagar H, Raghuwanshi N, Sharan S, Nikhil K, et al. Drug functionalized microbial polysaccharide based nanofibers as transdermal substitute. Nanomedicine. 2016;**12**(5):1375-1385. DOI: 10.1016/j.nano.2016.01.019

[158] Bonifacio MA, Cometa S, Cochis A, Gentile P, Ferreira AM, Azzimonti B, et al. Data on Manuka Honey/Gellan gum composite hydrogels for cartilage repair. Data in Brief. 2018;**20**:831-839. DOI: 10.1016/j.dib.2018.08.155

[159] Yu I, Kaonis S, Roland CR. A study on degradation behavior of 3D printed gellan gum scaffolds. Procedia CIRP. 2017;**65**:78-83. DOI: 10.1016/j.procir.2017.04.020

[160] Lin T, Lu C, Zhu L, Lu T. The biodegradation of zein in vitro and in vivo and its application in implants. AAPS PharmSciTech. 2011;**12**(1):172-176. DOI: 10.1208/s12249-010-9565-y

[161] Maharjan B, Joshi MK, Tiwari AP, Park CH, Kim CS. In-situ synthesis of AgNPs in the natural/synthetic hybrid

nanofibrous scaffolds: Fabrication, characterization and antimicrobial activities. Journal of the Mechanical Behavior of Biomedical Materials. 2017;**65**:66-76. DOI: 10.1016/j.jmbbm.2016.07.034

[162] Zhang M, Li X, Li S, Liu Y, Hao L. Electrospun poly(l-lactide)/zein nanofiber mats loaded with Rana chensinensis skin peptides for wound dressing. Journal of Materials Science. Materials in Medicine. 2016;**27**(9):136. DOI: 10.1007/s10856-016-5749-7

[163] Figueira DR, Miguel SP, de Sá KD, Correia IJ. Production and characterization of polycaprolactone-hyaluronic acid/chitosan- zein electrospun bilayer nanofibrous membrane for tissue regeneration. International Journal of Biological Macromolecules. 2016;**93**(Pt A): 1100-1110. DOI: 10.1016/j.ijbiomac.2016.09.080

[164] Babitha S, Korrapati PS. Biodegradable zein-polydopamine polymeric scaffold impregnated with TiO2 nanoparticles for skin tissue engineering. Biomedical Materials. 2017;**12**(5):055008. DOI: 10.1088/1748-605X/aa7d5a

[165] Sultana N, Khan TH. In vitro degradation of PHBV scaffolds and nHA/PHBV composite scaffolds containing hydroxyapatite nanoparticles for bone tissue engineering. Journal of Nanomaterials. 2012;**2012**:190950. DOI: 10.1155/2012/190950

[166] Sundaramurthi D, Krishnan UM, Sethuraman S. Epidermal differentiation of stem cells on poly(3-hydroxybutyrate-co-3-hydroxyvalerate) (PHBV) nanofibers. Annals of Biomedical Engineering. 2014;**42**(12):2589-2599. DOI: 10.1007/s10439-014-1124-3

[167] Keshel SH, Biazar E, Rezaei Tavirani M, Rahmati Roodsari M, Ronaghi A, Ebrahimi M, et al. The healing effect of unrestricted somatic stem cells loaded in collagen-modified nanofibrous PHBV scaffold on full-thickness skin defects. Artif Cells Nanomed Biotechnol. 2014;**42**(3):210-216. DOI: 10.3109/21691401.2013.800080

[168] Zine R, Sinha M. Nanofibrous poly(3-hydroxybutyrate-co-3-hydroxyvalerate)/collagen/graphene oxide scaffolds for wound coverage. Materials Science & Engineering. C, Materials for Biological Applications. 2017;**80**:129-134. DOI: 10.1016/j.msec.2017.05.138

[169] Yuan J, Geng J, Xing Z, Shim KJ, Han I, Kim J, et al. Novel wound dressing based on nanofibrous PHBV-keratin mats. Journal of Tissue Engineering and Regenerative Medicine. 2015;**9**(9):1027-1035. DOI: 10.1002/term.1653

Chapter

Microfluidic Device for Single Cell Impedance Characterization

Muhammad Asraf Mansor and Mohd Ridzuan Ahmad

Abstract

Detection of single particle has emerged as a noninvasive technique for diagnostic and prognostic patients with cancer suspected. Microfluidic impedance cytometry has been utilized to detect and measure the electrical impedance of single biological particles at high speed. The detailed information of single cells such as cell size, membrane capacitance, and cytoplasm conductivity also can be obtained by impedance measurement over a wide frequency range. In this work, we developed an integrated microneedle microfluidic device to detect and discriminate 9- and 16-μm microbeads. Two microneedles were utilized as measuring electrodes at the half height of the microfluidic device to perform measurement of electrical impedance under a presence of cells at the sensing area. Furthermore, this device was able to distinguish the cell concentration in the suspension fluid. The reusable microneedles were easy to be inserted and withdrawn from the disposable microfluidic. The ultrasonic cleaning machine has been used to clean the reusable microneedle with a simple cleaning process. Despite of the low-cost device, its capability to detect single particles at the sensing area was preserved. Therefore, this device is suitable for cost-efficient medical and food safety screening and testing process in developing countries.

Keywords: impedance, flow cytometry, microfluidics, microneedle, single cell

1. Introduction

The single cell analysis (SCA) has been emphasized to provide biologists and scientists to peer into the molecular machinery of individual cells. For the application of medical diagnosis, detection of cancer cells and pathogenic bacteria cells in blood is utilized as a diagnosing infectious disease. It is reported that detection of circulating tumor cells (CTCs) in the blood has shown to be clinically important for early stage metastasis or recurrence of cancer. The presence of rare CTCs in blood is ranging from only 1–100 CTCs/ml blood [1]. *Plasmodium falciparum* malaria, which kills mainly children in developing countries infected the blood sample of patients at concentration of ~1/50 μl of blood [2]. Nowadays, the analysis of single cell in biological measurements and medical research has emerged as a distinct new field and acknowledged to be one of the fundamental building blocks of life [3]. Amongst of various single cell analysis, cell impedance measurement has become an effective method of biological measurement [4]. The physiological behavior of the cells and their corresponding molecular expressions have significant effect on the cell membrane and cytoplasm conductivity and dielectric constant, which in turn affects the overall impedance characteristics [5]. For that reason, the impedance

measurements on single cells can provide relevant information about its functional status and may be a simple and significantly less complex alternative to detailed molecular expression studies.

The classical method for cell detection in suspension is using flow cytometry, which is rapid and highly accurate measurement technique. Impedance flow cytometry is an indirect signal extraction from the single cells on microchannel sensing area without having direct access into intracellular region of the cells [6]. These techniques were first reported by Coulter [7] has emerged in the microfabrication device in order to analyze microscale particle with high sensitivity. However, flow cytometry involves expensive manufacturing and labelling of the cells with fluorescent antibodies [8]. Recently, the impedance flow cytometry (IFC) has gained attention for the significant promising techniques to replace and overcome the limitations associated with flow cytometry. The IFC is preferable because of fast, real-time, and non-invasive methods for biological detection. This technique is capable to be utilized as cell counting [8], cancer cell detection [9] and bacteria detection [10]. Some groups have demonstrated detection and counting of cells by using a microfluidic integrated with electrode for various electrical measurement methods in an application of food safety [11] and real-time monitoring bio-threat [12]. This measurement technique is based on the alteration of impedance across a measurement electrode due to the blocking of ionic current passing between electrodes when a presence of the cells.

The IFC is capable to distinguish and count lymphocytes, monocytes and neutrophils in human whole blood [8]. Other studies reported that IFC can detect the presence of cells based on probing the impedance inside the cell at frequency greater than 1 MHz [13]. Fabricated nanoneedles probe inside microfluidic was utilized for measuring the presence of cells at sensor surface and making it sensitive to the dielectric properties of solution [14]. However, this device requires patterning of electrode or probe on the substrate resulting in higher cost of the fabrication process. Another limitation also needs to consider is time-consuming cleaning process of the device. Several groups have demonstrated the technique to reduce the cost of microfabrication of electrodes by using printed circuit board (PCB) as a measurement electrode. They demonstrated contactless conductivity detection in capillary electrophoresis manners [15] and cell manipulation using dielectophoresis [16]. Recently, the contactless impedance cytometry was developed to reduce the fabrication cost of impedance cytometry device [17, 18]. The electrode was fabricated on the PCB substrate (reusable component) and the thin bare dielectric substrate bonded to a PDMS microchannel (disposable component) was placed onto PCB substrate. The sensitivity of this device is the limitation since the electric field was buried in dielectric substrate and not reaches the electrolyte. Several designs and method in IFC in order to detect and analyze a cell have been reported [19, 20].

This chapter discusses a novel integrated microneedles-microfluidic system for detecting yeast cell concentration in suspension as well as detecting a single particle based on the impedance measurement. The development of the device focuses on reducing the fabrication cost while preserving the main functionality, that is, cell detection. The significant fabrication cost reduction in this work is by replacing the microfabrication of electrodes by the microneedles. This device utilized a Tungsten microneedle as a measurement electrode which can be reused and easily to be cleaned. The two microneedles were placed at half height disposable microchannel to detect and enable impedance measurement of passing cells through the applied electric field. **Figure 1(a)** illustrated the schematic diagram of the proposed microfluidic chip which consists of two microneedles integrated at both sides of the microchannel. The main sensing area microchannel length, width and thickness are

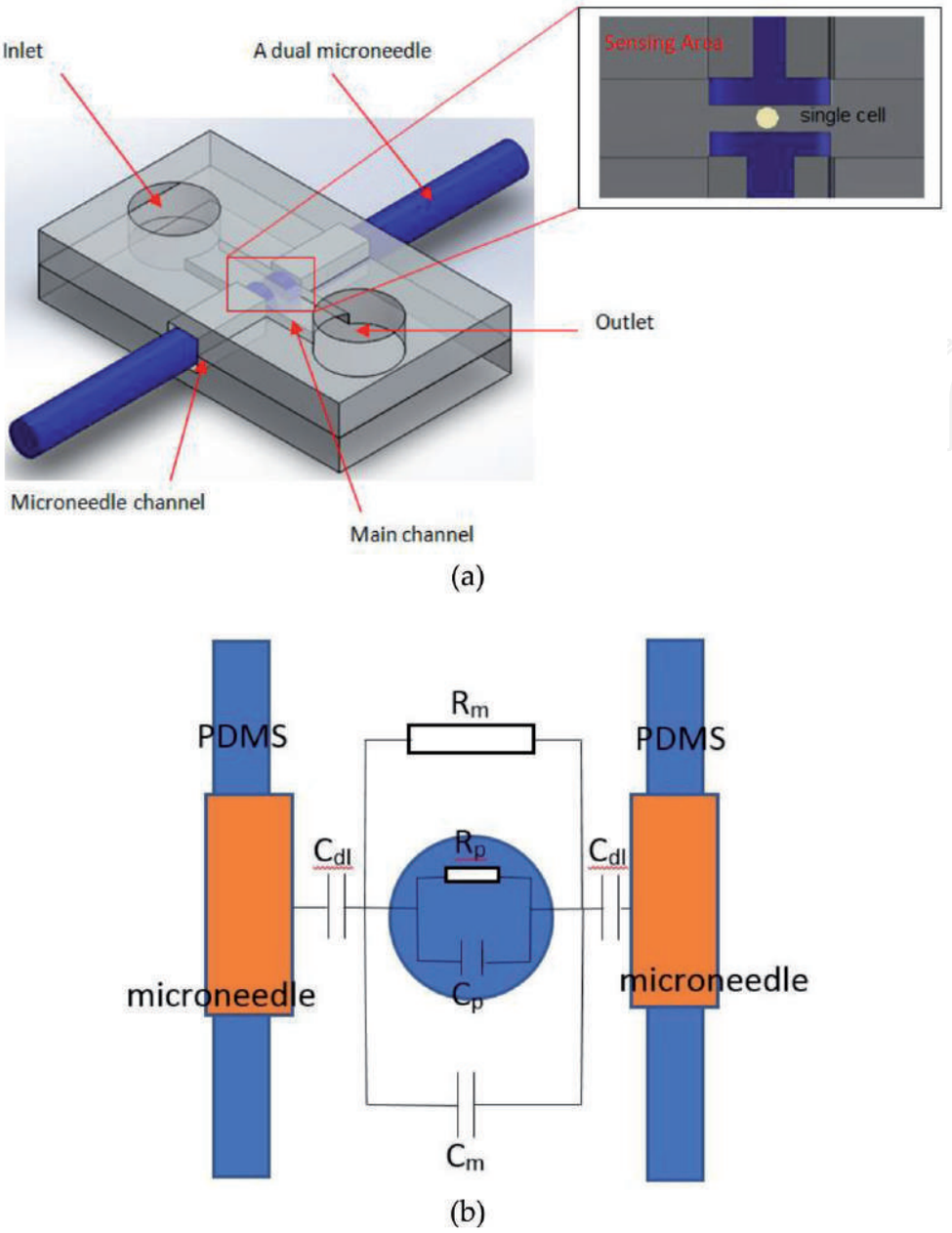

Figure 1.
(a) 3D schematic diagram of the microfluidic device structure integrated with microneedle and top view of sensing area which the impedance measurement of single particle be measured. (b) Microfluidic sensing area equivalent circuit model.

100, 25 and 25 μm respectively. The device is suitable for early cancer cell detection application in developing countries since it significantly reduces the fabrication cost, that is, not required the fabrication of micro electrode.

1.1 Principle

Ohm's Law has been use as the basic principle of detecting suspended biological cells in the media. The passing cells across the sensing area have been measure by an AC current with a frequency sweep to determine the changing impedance value of media. **Figure 1(b)** illustrated the equivalent circuit model for obtain the all parameter involved in order to characterize the electrical properties of cell between two microneedles in the suspension media. The sensing area of mirofluidic chip can be modeled electrically as cell impedance of resistance R_p and cell capacitance C_p in parallel with the impedance contributed by all materials between the two

electrodes, which consist solution resistor R_m in parallel with solution capacitance C_m. Both impedance in series with a pair of electrodes capacitance double layer C_{dl}. Z_T is overall impedance of the measurement system given [21].

$$Z_T = \frac{2}{j\omega C_{dl}} + \frac{R_m R_p}{R_m + R_p + j\omega R_m R_p (C_m + C_p)} \quad (1)$$

where ω is the angular frequency of the electrical signal. As a result, the Z_T is changing according the present of cell in the sensing area. The impedance between electrode (microneedle) and electrolyte (solution medium) is our main focus in this work.

1.2 Experimental works

1.2.1 Cell culture

In this work, Sacharomycesceresiae cells and microparticle are used as a model for proof of concepts. Sacharomycesceresiae were cultivated in a petri dish containing 10 ml of YPD broth (Yeast extract Peptone Dextrose). The YPD broth contained 1% yeast extract, 2% peptone and 2% glucose. The YPD dishes were incubated at 37°C for 24 hours. The cells were washed with deioinsed (DI) water three times by centrifugation, then they were suspended in sterilized deioinsed water at various dilutions (1:10) concentration. The cells were incubated on agar plates at 37°C for 24 hours for determining the number of cells. The diameter of yeast cells varies from 4 to 7 μm. The number of cells was 1.3×10^9 colony forming units per milliliter (cfu/ml). The conductivity of DI water is 6 mS/m. The non-fluorescent polystyrene (PS) microbeads with diameter 15 and 9 μm (Polysciences. Inc.) suspended in Phosphate-buffered saline (PBS) solution were diluted to a final concentration of 1000 beads per ml. Polystyrene beads have a known size and electrical properties [22] and have constant impedance across the frequency range used in these experiments.

1.2.2 Device fabrication

The photolithography technique was utilized to fabricate the microfluidic device. The fabrication begins by designing the masks using layout editor software. The laser lithography system (μPG501, Heidelberg Instruments, Germany) has been used to write the two masks (top and bottom) on the chromium (Cr) masks. Two-step photolithography using SU-82025 negative photoresist (MicroChem, USA) was utilized to fabricate the top layer mold. The first layer has a thickness of 25 μm and was spin coated onto a silicon substrate. After pre-baking, the top layer of Cr mask was place onto the first layer of photoresist for pattern transfer by using a mask aligner (SussMicroTech MA-6), then post-baking with development. Next, the second layer with 60 μm thickness was spin coated on the first photoresist layer and pre-baking. Then, the second layer of photoresist substrate was exposed with the bottom layer Cr mask by UV light. After exposed, the top mold master was obtaining by post-bake and developed process. Meanwhile the bottom mold master with 60 μm thickness was fabricated by following the SU-8 microchannel photolithography technique. PDMS pre-polymers (SYLGARD184A) was thoroughly mixing with curing agents (SYLGARD 184B) in a ratio of 10:1 by weigh for fabricate the PDMS microfluidic chip. The mixing PDMS was poured on an SU-8 mold master (top and bottom mold master) and left for whole night cured at room temperature to obtain the PDMS microfluidic chip. To increase the bonding strength between the top side and bottom side of PDMS microfluidic chip, they were cleaned with Isopropyl alcohol (IPA) and treated by Oxygen plasma (Plasma Etch PE-25) for 25 seconds [23]. The bonding

process of both side PDMS microfluidic chip was completed in less than 2 minutes to prevent loss of Oxygen plasma effectiveness. Finally, the right and left sides of the microchannel chip were cut and leaving a square (60 μm × 120 μm) hole for inserting a microneedle. For measuring electrode, two Tungsten microneedle (Signatone) coated by parylene with tip diameter, shank diameter and length of tungsten needle are 25, 250 and 31.7 mm, respectively, was utilized.

1.2.3 Device operation

The microscope (Olympus Inverted Microscopes IX71) was utilized to monitor the sensing area of microfluidic chip system. The micromanipulator (EB-700, Everbeing) was utilized to insert the two microneedles into microchannel chip through the square hole at right and left side of the chip. For this experiment, the gap between microneedles was fixed at 20 μm. **Figure 2** illustrated the experimental setup of impedance measurement. The two microneedles were connected to impedance analyzer (Hioki IM3570) for input measuring and the result was displayed on the computer. Then, by controlling the syringe pumps (KDS LEGATO 111, KD Scientific, and USA), the 3-ml syringes of the sample solution and yeast concentration was introduced into microfluidic chip via two tygon flexible tubes.

1.2.4 Impedance measurement procedure

Standard short and open self-calibration procedure has been used for impedance analyzer in order to perform the impedance measurement. Furthermore, to calibrate the chip, impedance of 1xPBS solution was measured at the 20 μm of electrode gap. Three microfluidic devices were utilized for reproducibility testing and the experiments were conducted at room temperature. To validate the equivalent circuit model, impedance of the medium between microneedle was measured. The solutions were sterilized DI water and PBS (Photosphate-buffered saline) with conductivities 6 and 1.4 S/m respectively.

Initially, 1 ml of PBS with concentrations of 1500 mOsm was prepared for the chip cleaning process. The sample was loaded into a syringe and driven through the microchannel using a syringe pump with the flow rate of syringe pump was kept constant (60 μl/min). After flushing with PBS solution, yeast cell of 1 ml of each seven different concentrations of sample from 10^2 to 10^9cfu/ml were driven

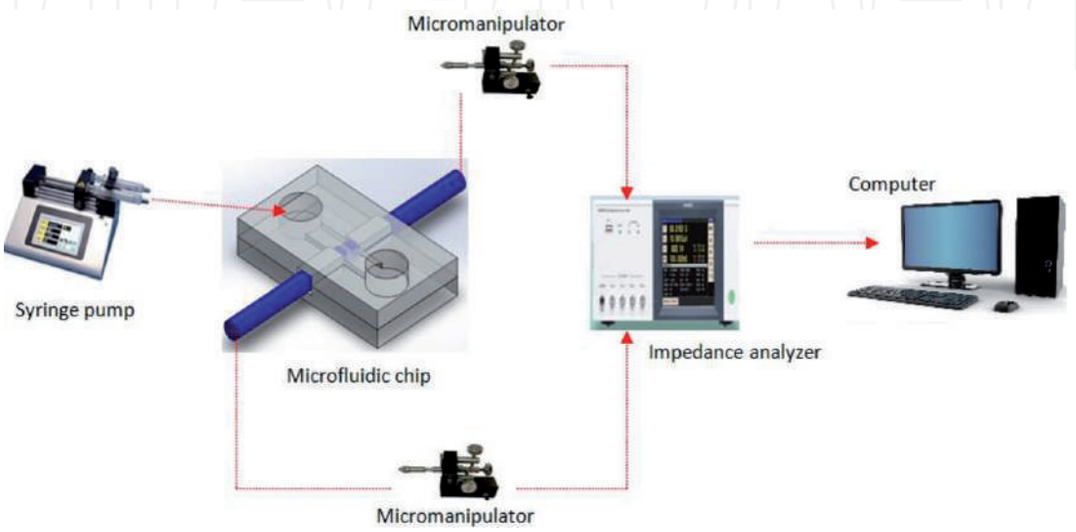

Figure 2.
The experimental set-up diagram.

through the microchannel at a flow rate of 6 μl/min. The impedance of each solution was measure by connecting the microneedles with impedance analyzer. Then, an AC signal frequency range from 100 Hz to 5 MHz with an applied voltage of 1 V was apply to determine the impedance spectra (impedance and phase vs. frequency) in order to differentiate the variations of solution samples. Between each sample measurement, the microchannel chip was flushed by DI and PBS water for 1 and 2 minutes respectively. The impedance analyzer (Hioki IM3570) GUI and post-processed in MATLAB (MathWorksInc, USA) was utilized to record the data. The impedance change during the passage yeast cells at sensing area was measured. In order to monitor the behavior of impedance for each sample, the impedance value at three frequencies (100 kHz, 500 kHz and 1 MHz) was measured.

Single cell detection and measurement was conducted based on impedance measurement with or without single cell at the sensing area. Two sample of microbeads with diameter 15 and 9 μm suspended in 1 ml of PBS with concentration of 10^3 per ml were utilized to perform this measurement and detection. Each sample were driven through the microchannel at a flow rate of 6 μl/min and measured using an AC signal frequency range from 100 Hz to 5 MHz.

1.3 Result and discussion

As a proof of concepts, the dependencies of the impedance on the various concentrations of yeast cells and a single microbead in the suspension medium by using this microfluidic device are studied. **Figure 3** presents the measured impedance spectra and fitting spectra (on a log scale) of the system for two of microchannel filled with sterilized DI water and PBS at frequency range 1 kHz to 1 MHz. For simulation, 100 data points on the impedance measured spectrum were used as input to the equivalent circuit [see **Figure 1(b)**] and generating the fitting impedance spectrum by using MATLAB. For high conductivity fluid (PBS), the result shows two domains which were an electrical double layer (EDL) region and a resistive region [24]. The EDL occurred in the low frequency range from 1 kHz to approximately 300 kHz, whereas the resistive region occurred in high frequency from 300 kHz to 1 MHz. The agreement between the measured and fitting spectra result indicated that our developed circuit model for this system is feasible to determine the impedance characteristics of solution medium.

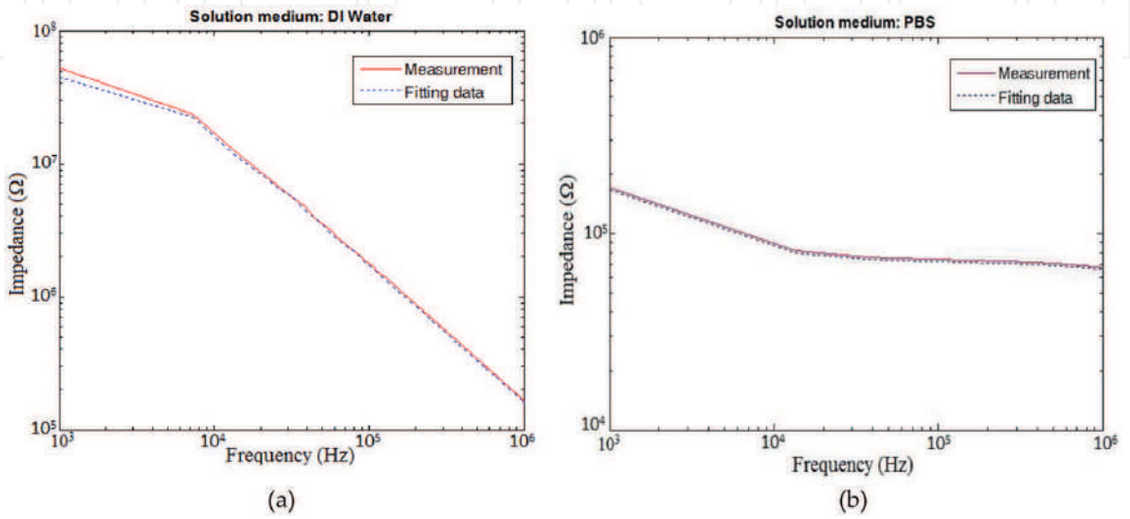

Figure 3.
Impedance spectra of sample solution together with their fitting spectra: (a) DI water (b) PBS.

To illustrate the cell detection capability of the device, yeast cell and microbeads with different concentration was utilized. Yeast cells concentration ranging from 10^2 to 10^9 cfu/ml were infused inside microchannel with fixed flow rate 6 μl/min and fixed electrode gap (25 μm). A sweep frequency (100 kHz to 5 MHz) AC signal (1 V) was applied to the one side of the microneedle and the current entering at another side of microneedle was measured to calculate the impedance of concentration of yeast cells in DI water. Initially, 10^9 cfu/ml was injected resulting in a drop-in impedance by referring the impedance of DI water as a control. Afterward, the microchannel chip was washed by the PBS followed by DI water at maximum flow rate.

The maximum flow rate of the liquid can flow inside microchannel without leaking is 300 μl/min. **Figure 4(a)** shows the impedance spectra of yeast cell in DI water with the different cell concentration in the range 10^4–10^9cfu/ml, along with DI water as a reference. After washing the microchannel, 10^8cfu/ml was infused to the microchannel resulting in an increase in impedance. It can be seen the impedance spectra of yeast cell in DI water across the sensing area (two microneedles)

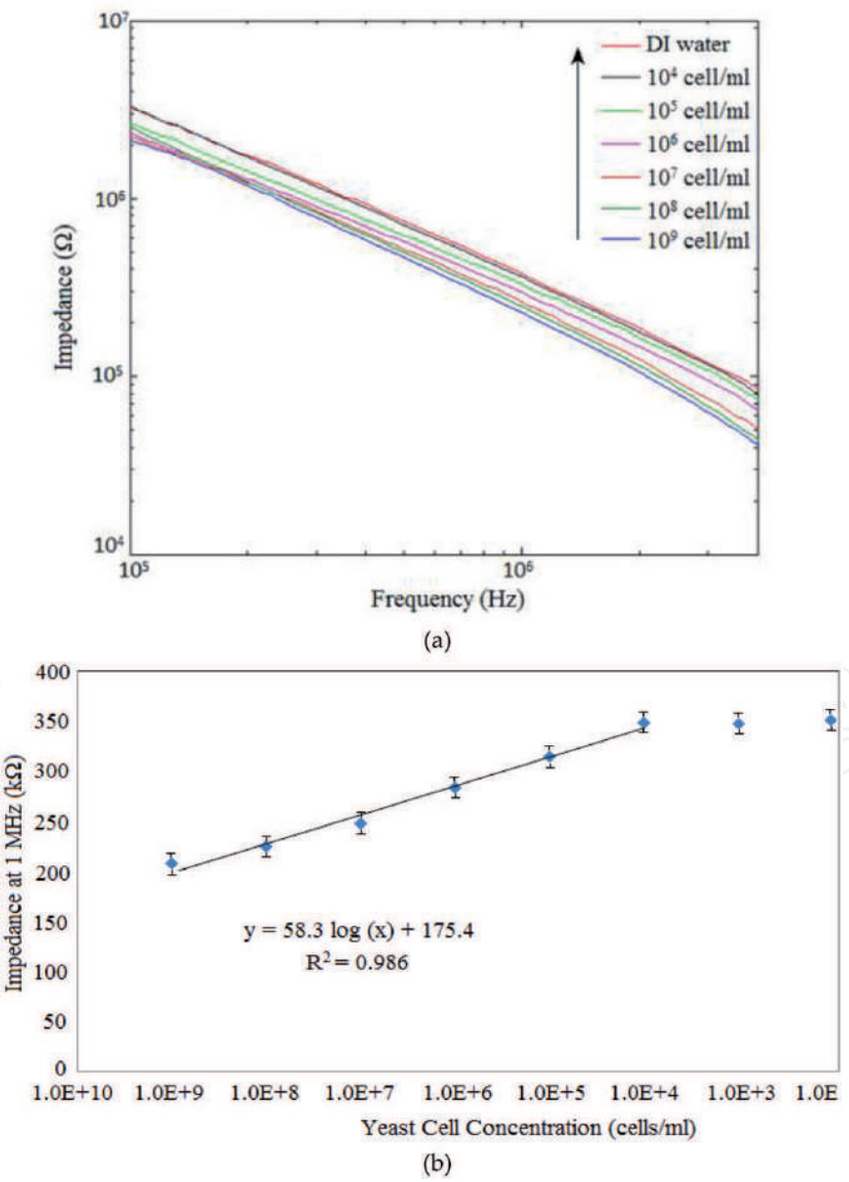

Figure 4.
(a) Impedance spectra of yeast cells in water with cell concentrations ranging from 10^2 to 10^9cfu/ml, along with DI water as controls; (b) the logarithmic value of the concentration of yeast cells and the impedance measured at 1 MHz with linear relationship.

increase with decreasing the cell concentration of cells [14]. According to the observation result, it can be said that cell suspension with high concentrations is more conductive than those with lower concentrations.

The conductivity of solution varies proportionally to the number of cell concentration at fixed volume of solution [25]. In some studies, the relative dielectric permittivity and charged polyelectrolytes inside the cell also may affect the impedance of solution [14]. The optimum region for sensing microneedle to differentiate the cell concentration in DI water occurs between 500 kHz to 5 MHz. The impedance values of the suspensions in this frequency region were significantly different from each other. The experiment was repeated two times measurement cycle and showed the similar result.

In cell detection experiment, frequency lower than 100 kHz are not considered, as the EDL started to influence the measurement at frequency below 300 kHz [17, 26]. In order to investigate the relationship between impedance value and cell concentration, we selected 1 MHz as the best representative frequency. **Figure 4(b)** illustrates the impedance responses of the sample containing different yeast cell concentrations and DI water at frequency measurement 1 MHz. The impedance of the solution was significantly increased from 207.63 to 225.42, 247.61, 284.48, 314.64, and 348.51 kΩ when the yeast concentration decreasing from 10^9 to 10^8, 10^7, 10, 10 and 10^4 cfu/ml respectively. After the cell concentrations were lower than 10^4 cfu/ml, impedance value shows no significant changing between each other or DI water. In additions, the pattern of the result shows a linear relationship between the impedance and the logarithmic value of the cell concentration at cell concentration from 10^4 to 10^9 cfu/ml (see **Figure 4**). The linear regression equation of this result is Z (kΩ) = 58.3 log X (cells/ml) + 175.4 with R2 = 0.986. The detection limit was calculated to be 1.2×10^4 cfu/ml. Error bars are standard deviations of five measurements cycle.

In order to measure the cell concentration in DI water suspensions, the linear regression equation of the impedance of the yeast suspensions was used. This device can be utilized to quantify cells in suspensions other than impedance microbiology and impedance biosensors for bacteria detection since the detection limit of this method is comparable with another sensor. The reported sensor for detection of pathogenic bacteria are QCM immunosensors for detection of Salmonella with detection limits of 9.9×10^5 cfu/ml [27], surface plasmon resonance (SPR) sensor for detection of *E. coli* O157:H7 with a detection limit of 10^7 cfu/ml [28] and SPR immounosensors for detection of Salmonella enteritidis and Listeria monocytogens with detection limits of 10^6 cfu/ml [29].

In order to demonstrate the capability of this device in detecting the present of single cell, two size of micro bead have been flowing inside the microfluidic device. The impedance of PBS solution as a control was initially infused inside the microfluidic device. Then two samples of microbeads in PBS solution were infused inside the microchannel with the same flow rate and electrode gap of yeast cell concentration measurement. **Figure 5(a)** shows the 15-μm microbead flow through the sensing area and a sweep frequency ranging from 100 kHz to 3 MHz AC signal (1 V) was applied to the electrode. As the result, the impedance spectrum is plotted over the field frequency, as shown in **Figure 5(b)**. The figure shows the average electrical impedance data for two size of beads and PBS solution without present of beads. From this average data, it is expected that the electrical impedance spectrum can be used to differentiate between the sizes of beads. The beads (9 and 15 μm in diameter) are clearly discriminated by impedance spectrum. The impedance increases with the increasing of the size of particle. Due to the presence of a single bead that can be regarded as an insulating object, the electrical resistance of the sensing channel was slightly increased.

As the result, we conclude this device can detect the cell concentrations in solution medium and the single microbead at the high frequency range between 100 kHz and 5 MHz. In this experiment, we did not determine the detection capability at the frequency lower than 100 kHz. For the future work, we will focus on the measurement and detection to the human cell (normal and cancer cell) the size of microneedle, single cell detection and utilize a non-polarizable electrode, that is, Ag/AgCl (to eliminate the EDL), in order to improve the performance of the device.

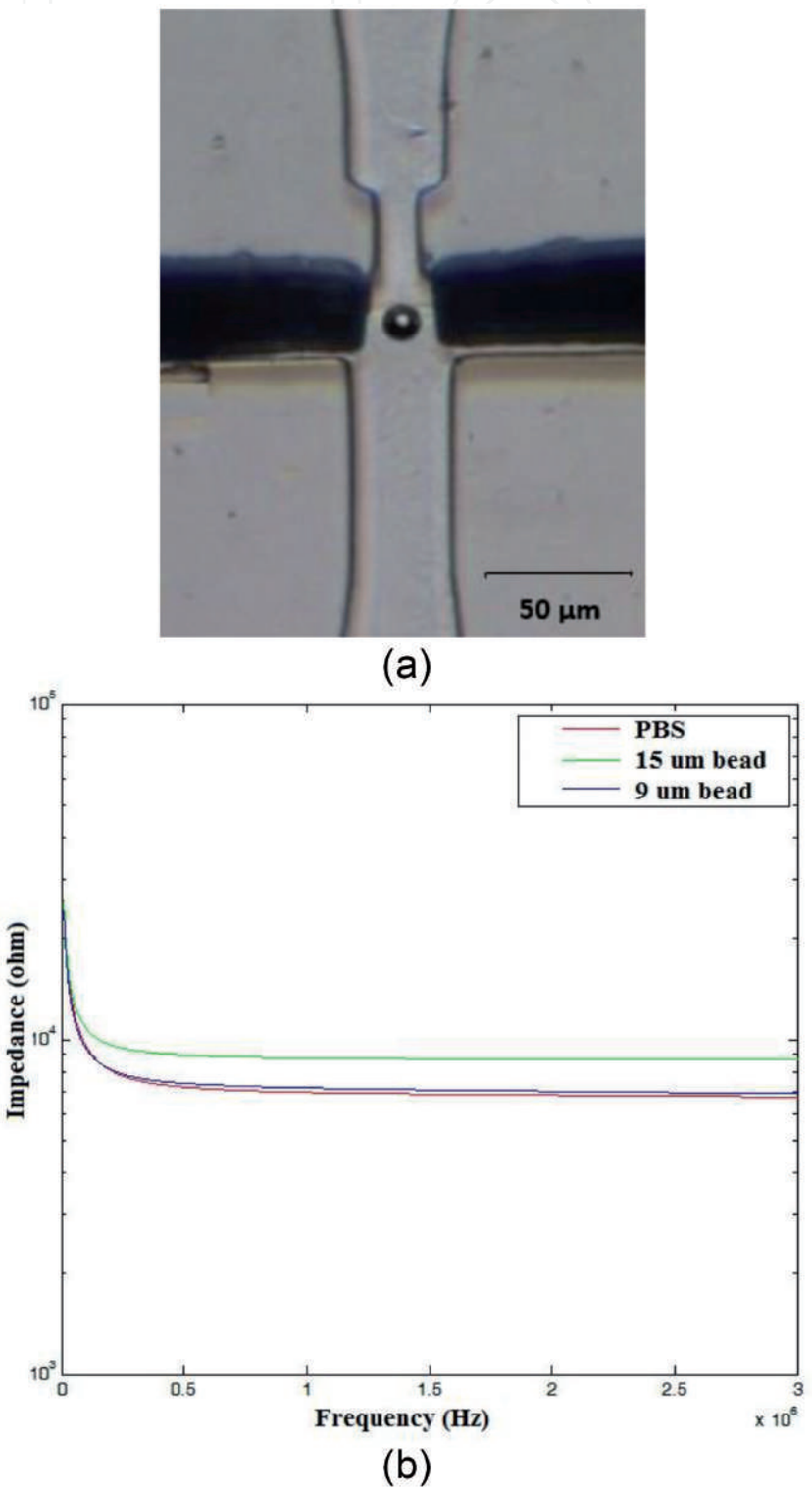

Figure 5.
(a) The single microbead with diameter of 15 µm flows through the sensing area. (b) Impedance spectrum of two different sizes of beads in PBS solution and PBS solution (without bead).

2. Conclusions

For conclusion, a simple, low-cost and label-free microfluidic device has developed to detect the cell concentration and single cell in the suspension medium. This device contains a disposable PDMS microchannel which allow a reusable microneedle insert into microchannel. The result demonstrated the increase of cell concentration in the solution medium were decrease the impedance value. The capability of this device to differentiate the concentration of cell from 10^9 to 10^4 cfu/ml shows the core functionality of the proposed sensor even though the manufacturing cost was significantly lower. In addition, the microfluidic device capable to detect single cell and decimate the size of single cell. As a proof of concept, yeast cell and microbeads were used in this study and we emphasize this sensing technique can be applied to a variety of cell types with diameter size in a range from 5 to 25 μm. It is recommended to perform only one measurement time for each PDMS microchip in order to avoid the potential spread of contamination to samples. The fabrication cost of this device is significantly reduces (≈ 30% fabrication cost was reduced based on facility rental and raw material usage) which is suitable for early cancer cell detection and water contamination application in developing countries.

Acknowledgement

The research was supported by the Ministry of Higher Education of Malaysia and Universiti Teknologi Malaysia (Grant Nos. Q.J130000.21A2.03E11 and Q.J130000.2423.03G47); we thank them for funding this project and for their endless support.

Author details

Muhammad Asraf Mansor and Mohd Ridzuan Ahmad*
Micro-Nano System Engineering Research Group, Faculty of Engineering, Division of Control and Mechatronic Engineering, School of Electrical Engineering, Universiti Teknologi Malaysia, Skudai, Johor, Malaysia

*Address all correspondence to: mdridzuan@utm.my

References

[1] Kantara C et al. Methods for detecting circulating cancer stem cells (CCSCs) as a novel approach for diagnosis of colon cancer relapse/metastasis. Laboratory Investigation. 2015;**95**(1):100-112

[2] Ciceron L, Jaureguiberry G, Gay F, Danis M. Development of a plasmodium PCR for monitoring efficacy of antimalarial treatment. Journal of Clinical Microbiology. 1999;**37**(1):35-38

[3] Gilchrist KH et al. General purpose, field-portable cell-based biosensor platform. Biosensors & Bioelectronics. 2001;**16**(7-8):557-564

[4] Jao J-Y, Liu C-F, Chen M-K, Chuang Y-C, Jang L-S. Electrical characterization of single cell in microfluidic device. Microelectronics and Reliability. 2011;**51**(4):781-789

[5] Yang L, Arias LR, Lane TS, Yancey MD, Mamouni J. Real-time electrical impedance-based measurement to distinguish oral cancer cells and non-cancer oral epithelial cells. Analytical and Bioanalytical Chemistry. 2011;**399**(5):1823-1833

[6] Sun T, Morgan H. Single-cell microfluidic impedance cytometry: A review. Microfluidics and Nanofluidics. 2010;**8**(4):423-443

[7] Coulter WH. High speed automatic blood cell counter and cell analyzer. Proceedings of the National Electronic Conference. 1956;**12**:1034-1040

[8] Holmes D, Morgan H. Single cell impedance cytometry for identification and counting of CD4 T-cells in human blood using impedance labels. Analytical Chemistry. 2010;**82**(4):1455-1461

[9] Gou H-L, Zhang X-B, Bao N, Xu J-J, Xia X-H, Chen H-Y. Label-free electrical discrimination of cells at normal, apoptotic and necrotic status with a microfluidic device. Journal of Chromatography. A. 2011;**1218**(33):5725-5729

[10] Du E, Ha S, Diez-Silva M, Dao M, Suresh S, Chandrakasan AP. Electric impedance microflow cytometry for characterization of cell disease states. Lab on a Chip. 2013;**13**(19):3903-3909

[11] Liu Y-S, Banada PP, Bhattacharya S, Bhunia AK, Bashir R. Electrical characterization of DNA molecules in solution using impedance measurements. Applied Physics Letters. 2008;**92**(14):143902

[12] Javanmard M, Talasaz AH, Nemat-Gorgani M, Pease F, Ronaghi M, Davis RW. Targeted cell detection based on microchannel gating. Biomicrofluidics. 2007;**1**(4):1-10

[13] Gawad S, Schild L, Renaud PH. Micromachined impedance spectroscopy flow cytometer for cell analysis and particle sizing. Lab on a Chip. 2001;**1**(1):76-82

[14] Esfandyarpour R, Javanmard M, Koochak Z, Harris JS, Davis RW. Nanoelectronic impedance detection of target cells. Biotechnology and Bioengineering. 2014;**111**(6):1161-1169

[15] Wang J, Chatrathi MP, Mulchandani A, Chen W. Capillary electrophoresis microchips for separation and detection of organophosphate nerve agents. Analytical Chemistry. 2001;**73**(8):1804-1808

[16] Park K, Suk H-J, Akin D, Bashir R. Dielectrophoresis-based cell manipulation using electrodes on a reusable printed circuit board. Lab on a Chip. 2009;**9**(15):2224-2229

[17] Emaminejad S, Javanmard M, Dutton RW, Davis RW. Microfluidic

diagnostic tool for the developing world: Contactless impedance flow cytometry. Lab on a Chip. 2012;**12**(21):4499

[18] Emaminejad S, Paik K, Tabard-Cossa V, Javanmard M. Portable cytometry using microscale electronic sensing. Sensors and Actuators B: Chemical. 2016;**224**:275-281

[19] Mansor MA, Ahmad MR. Single cell electrical characterization techniques. International Journal of Molecular Sciences. 2015;**16**(6):12686-12712

[20] Mansor MA, Ahmad MR. A simulation study of single cell inside an integrated dual Nanoneedle-microfluidic system. Jurnal Teknologi. 2016;**78**(7-5):59-65

[21] Sun T, Holmes D, Gawad S, Green NG, Morgan H. High speed multi-frequency impedance analysis of single particles in a microfluidic cytometer using maximum length sequences. Lab on a Chip. 2007;**7**(8):1034-1040

[22] Spencer D, Hollis V, Morgan H. Microfluidic impedance cytometry of tumour cells in blood. Biomicrofluidics. 2014;**8**(6):064124

[23] Mansor M, Takeuchi M, Nakajima M, Hasegawa Y, Ahmad M. Electrical impedance spectroscopy for detection of cells in suspensions using microfluidic device with integrated microneedles. Applied Sciences. 2017;**7**(2):170

[24] Morgan H, Sun T, Holmes D, Gawad S, Green NG. Single cell dielectric spectroscopy. Journal of Physics D: Applied Physics. 2007;**40**:61-70

[25] Yang L. Electrical impedance spectroscopy for detection of bacterial cells in suspensions using interdigitated microelectrodes. Talanta. 2008;**74**(5):1621-1629

[26] Segerink LI, Sprenkels AJ, ter Braak PM, Vermes I, van den Berg A. On-chip determination of spermatozoa concentration using electrical impedance measurements. Lab on a Chip. 2010;**10**(8):1018

[27] Park IS, Kim WY, Kim N. Operational characteristics of an antibody-immobilized QCM system detecting salmonella spp. Biosensors & Bioelectronics. 2000;**15**(3-4):167-172

[28] Fratamico PM, Strobaugh TP, Medina MB, Gehring AG. Detection of Escherichia coli 0157:H7 using a surface plasmon resonance biosensor. Biotechnology Techniques. 1998;**12**(7):571-576

[29] Koubová V et al. Detection of foodborne pathogens using surface plasmon resonance biosensors. Sensors and Actuators B: Chemical. 2001;**74**(1-3):100-105

Chapter

Assessing the Vascular Deformability of Erythrocytes and Leukocytes: From Micropipettes to Microfluidics

Mark D. Scott, Kerryn Matthews and Hongshen Ma

Abstract

Among the most crucial rheological characteristics of blood cells within the vasculature is their ability to undergo the shape change (i.e., deform). The significance of cellular deformability is readily apparent based solely on the disparate mean size of human erythrocytes (~8 μm) and leukocytes (10–25 μm) compared to the minimum luminal size of capillaries (4–5 μm) and splenic interendothelial clefts (0.5–1.0 μm) they must transit. Changes in the deformability of either cell will result in their premature mechanical clearance as well as an enhanced possibility of intravascular lysis. In this chapter, we will demonstrate how microfluidic devices can be used to examine the vascular deformability of erythrocytes and agranular leukocytes. Moreover, we will compare microfluidic assays with previous studies utilizing micropipettes, ektacytometry and micropore cell transit times. As will be discussed, microfluidics-based devices offer a low-cost, high throughput alternative to these previous, and now rather ancient, technologies.

Keywords: deformability, hemorheology, red blood cells, white blood cells, micropipette assay, ektacytometry, cell transit analysis, microfluidic analysis, transfusion medicine

1. Introduction

The circulating cellular elements of blood consist of erythrocytes (red blood cells; RBC), leukocytes (white blood cells; WBC) and platelets. The hemorheology of these blood cells is unique in that these cells exist in a fluid phase subjected to variable, and often extreme, rheological shear stress, viscosity changes and biomechanical obstacles (e.g., capillaries and splenic filtration). Hemodynamically, shear stress is induced by the highly variable flow rate of blood within the ~100,000 kilometers of the human vasculature bed which encompasses both large arteries and veins to the capillary beds (**Figure 1A**) [1]. With an average resting cardiac output of approximately 5 L/min, blood flow in the largest artery (i.e., aorta) is approximately 50 cm/s while flow rates drop to only about 0.03 cm/s in the smallest capillaries and return to about 15–40 cm/s in the largest veins (e.g., superior and inferior vena cava) [1, 2]. In high flow conditions, RBC reside in the fast flowing central axial column of the vessel while WBC (and platelets) are located more peripherally

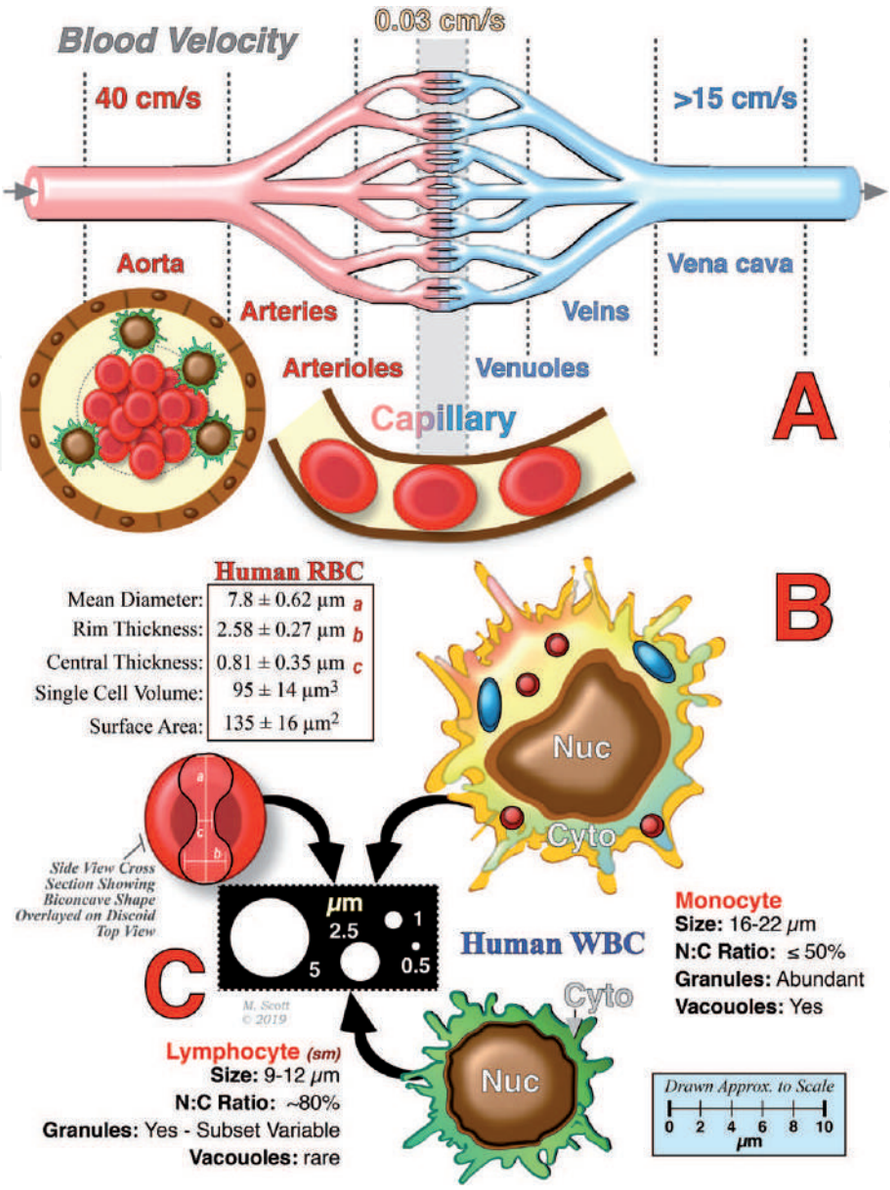

Figure 1.
The physiology and morphology of the vascular bed and blood cells imparts unique rheological stress on circulating blood cells. Panel A: the vascular bed is composed of blood vessels of various sizes which create significant disparity in blood (fluid and cellular) velocity consequent to vessel diameter. The fluid flow induces rheological sheer stress while the vessel size can create biomechanical deformation of cellular elements. Panel B: shown are the general physical parameters of human RBC and WBC. Note that the biconcave RBC is a anuclear while within the WBC, the nucleus:cytoplasm (N:C) ratio of monocytes and lymphocytes are quite divergent. RBC cytoplasmic viscosity is primarily defined by hemoglobin while in WBC, in addition to the nucleus, the presence of granules and vacuoles also impact intracellular viscosity and the aggregate cellular deformability. Panel C: blood cell deformability is crucial during vascular flow due to the size disparity between red blood cells and various leukocytes (e.g., monocytes and lymphocytes) and the capillary (4–58 µm) and splenic interendothelial clefts (0.5 µm). Panels B,C are drawn approximately to scale.

and prone to mechanical interaction with the endothelial cells lining the blood vessels. WBC also have adhesion molecules on their membrane and, if appropriate signals (e.g., inflammation) are present, they actively roll on the endothelial cells prior to attachment and extravasation (**Figure 1A,B**). Moreover, the viscosity of blood is also variable and is a function of, primarily, red blood cell (RBC) number and flow rate. At high RBC counts and high flow rates, blood is highly viscous while at low RBC counts and low flow rates (capillaries), blood viscosity is greatly reduced. Moreover, as shown in **Figure 1C**, the rheological stress is further exacerbated by the biomechanical stresses induced by the extreme disparity in the size of RBC (~8 µm) and WBC (10–25 µm) to the minimum diameter of the vascular

capillary beds (4–5 μm) and splenic interendothelial clefts (0.5–1.0 μm) [3, 4]. Hence, consequent to both the shear forces, viscosity and biomechanical stresses placed on blood cells, a key biologic/physiologic requirement of both RBC and WBC within the vascular space is rheological deformability. Biomechanically, the intracellular viscosity and membrane rigidity of the RBC and WBC are the key factors in imparting their vascular rheological deformability.

For the anuclear RBC, intracellular viscosity is primarily determined by hemoglobin content (both absolute content and hemoglobin structure (**Figure 1B**)). RBC membrane deformability/flexibility is primarily imparted by the cytoskeletal structure of the cells and, to a lesser extent, the composition of the bilayer itself (lipid species, protein content, integral versus peripheral membrane proteins, and carbohydrates). For normal RBC the intra- and inter-individual variability of both intracellular viscosity is relatively invariant; however, genetic mutations affecting hemoglobin structure (e.g., HbS, α and β thalassemia, HbE mutations) will dramatically affect both hemoglobin content and the viscosity of the hemoglobin itself. Similarly, the cytoskeletal structure of normal red blood cells is both well characterized and consistent within humans. But, as with hemoglobin variants, mutations in any component of the cytoskeleton can dramatically affect the discoid shape of the RBC and result in size changes and/or altered rigidity or stability of the cytoskeleton and cell itself. Indeed, numerous studies have documented that changes in either the hemoglobin content or structure (the major determinant of viscosity) or mutations to cytoskeletal components (the major determinant of membrane rigidity) can exert significant effects on RBC deformability, biologic function and in vivo circulation. In evidence of this, both biological conditions and pharmacologic agents that affect hemoglobin content and/or viscosity or the RBC cytoskeleton alter cellular deformability and have profound in vivo and in vitro effects on RBC function and survival [5–16]. Indeed, RBC deformability can be a diagnostic indicator of RBC abnormalities and the quality of stored RBC prior to transfusion [17–28].

Intracellular viscosity and membrane structure are similarly key to the rheological deformability of WBC. However, in contrast to RBC, WBC intracellular viscosity is more complex and affected by multiple components including the: nuclear to cytoplasm (N:C) ratio; intracellular granule composition; presence of cytoplasmic vacuoles; as well as the activation state of the immune cell (**Figure 1B**) [28–30]. Similarly, membrane rigidity is also more complex due to: abundance of membrane proteins and protein rafts; changes in protein structure and polymerization consequent to immune activation; and the variability of the membrane and cytoskeletal protein composition of immune cell populations (e.g., monocytes, lymphocytes, granulocytes) and subsets (e.g., T cells versus B cells; CD4+ versus CD8+ T cells; NK cells) [30–35]. Perhaps surprisingly, despite the biologic importance of its rheological deformability within the vasculature, WBC deformability is both poorly defined and much less understood. Indeed, previous studies on WBC have most commonly defined "deformability" as cellular shape change or spreading under extrinsic suction (e.g., micropipette aspiration), compression pressure (e.g., centrifugation and cell poker/probe), or upon activation induced motility [30–32, 34–36]. However, vascular deformability is vastly different from cellular shape change or spreading which are most commonly induced by immune cell activation and, importantly, the actual loss of vascular rheologically-mediated (i.e., fluid motion and spatial confinement) deformability. The paucity of data relating to vascular deformability of WBC has, in large part, been due to the absence of suitable tools for measuring deformability across the broad range of cell types encompassed within leukocyte population. However, the complexity of the leukocyte population and resultant changes in rheological deformability upon activation (e.g., granule

release) potentially arising in peripheral blood WBC may be of clinical importance as a biomarker of acute or chronic immune activation.

2. Measuring the vascular (rheological) deformability of blood cells

Because of the crucial role that cellular deformability plays in vascular circulation of RBC, methods to quantitate this biomechanical-aspect of normal and abnormal RBC has been of interest to hematologists since the 1960s [3, 5–7, 9, 10, 37–40]. Historically, multiple technological tools have been employed to study RBC (but rarely WBC) deformability including: micropipette aspiration; ektacytometry; cell transit times; and, most recently, microfluidic analysis.

2.1 Micropipette aspiration

Perhaps the earliest experimental approach to measure RBC deformability was the micropipette aspiration (**Figure 2**). Initial studies examined the ability of normal and stored RBC to traverse the length of a micropipette of known diameter [38]. This early "microfluidic" single cell analytical approach, while very low throughput and time consuming, did demonstrate that damaged or stored RBC were less deformable than fresh normal RBC. Subsequent variations of these micropipette studies further examined the localized elasticity of the membrane in both intact cells and RBC ghosts using ever smaller micropipettes to deform a small segment of the membrane to characterize static deformability via membrane extensional rigidity and bending rigidity. To further characterize dynamic deformability of the cells, the time constants for rapid elastic recovery from extensional and bending deformations were also quantitated [41–47]. However, micropipette, single-cell aspiration, measurements did not adequately reflect the biomechanical heterogeneity of even a relatively homogenous cell population (e.g., normal RBC), much less, the highly divergent population of cells encompassed within the WBC population. Hence newer methods were devised in an attempt to study large number of RBC under flow-like conditions. In contrast to RBC, micropipette studies are still commonly used to examine leukocytes; though these approaches tend not to be focused on rheological deformability [22, 35, 48–53].

2.2 Ektacytometry

Perhaps the most glaring flaw of the various micropipette aspiration approaches were their limitation to single cell analyses. To overcome this limitation, ektacytometry

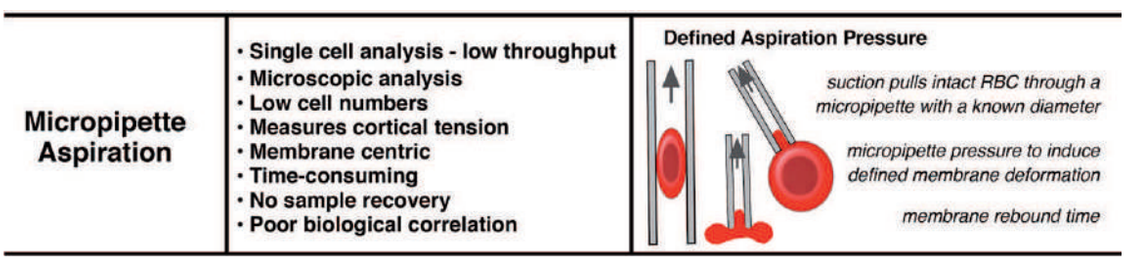

Figure 2.
Overview of micropipette aspiration analysis of blood cells. Micropipette-based analyses were first used to explore the crucial role of cellular deformability in the circulation of red blood cells. As noted, these single cell analyses were low throughput and time consuming. Multiple variation of this technique have been developed ranging from whole cell aspiration to localized membrane deformation. Studies could be done on intact cells or membrane ghosts.

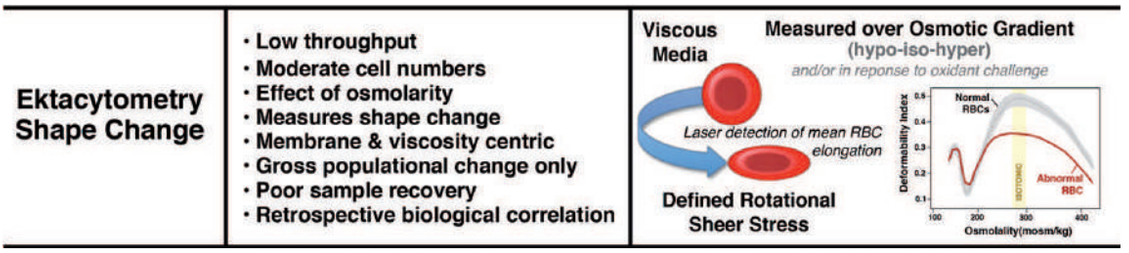

Figure 3.
Overview of ektacytometric analysis of blood cells. To overcome the single cell limitations inherent to micropipette aspiration, the ektacytometer can analyze the shear-induced deformability of a much larger population of RBC; though at the expense of information of single cell data acquisition. Ektacytometry measures deformability by subjecting RBC suspended in a viscous solution to rotational shear stress such that the normal cells form ellipsoids. The scatter intensity pattern from laser diffraction produces isointensity curves and deformability indices. Additionally, the most common approach of ektacytometry examines RBC deformability over a broad osmotic gradient (hypotonic → isotonic → hypertonic). Deformability is measured via laser diffraction as the shear stress forces the RBC to assume an elongated shape.

was developed. Ektacytometry measures deformability by suspending RBC in a viscous solution and applying rotational shear stress such that the normal discoid cells form ellipsoids which is measured by laser diffraction (**Figure 3**) [13, 14, 54–57]. The extent of ellipsoid formation is dependent on the deformability of the sample population. Abnormal RBC can be detected by shifts relative to the scatter intensity pattern of normal cells. Abnormal (i.e., non-deformable) cells can result in any combinations of left or right shifts in response to hypo- or hypertonicity, and/or a decrease in the maximum deformation observed under isotonic conditions. Relative to micropipette studies, ektacytometry provided a relative rapid assay to examine RBC. Numerous ektacytometry studies have elucidated the profound influence that mean corpuscular hemoglobin concentration (hence intracellular viscosity), abnormal hemoglobins, cytoskeletal aberrations, drugs and oxidant challenge exert on the cellular deformability [13, 14, 18, 54–64]. Importantly, ektacytometry only measures the "average deformability" of a cell population and cannot accurately and efficiently quantify the abundance of rigid cells in a bimodal population where both normal and abnormal cells are present [57, 65]. In the context of blood banking, ektacytometry has been used for assessing RBC following blood bank storage [66–68]. Of note, ektacytometry has been used exclusively in the context of erythrocytes; with no known studies examining the shear-induced deformability of lymphocytes, neutrophils, monocytes or other leukocytes. Thus, despite some promising data regarding its clinical use in transfusion medicine, ektacytometry has not become commonly used in transfusion medicine due to both the cost of instrumentation and the relatively low throughput of the existing testing protocols. Moreover, ektacytometry does have some significant drawbacks as it cannot, without experimental manipulations (e.g., density separation), provide any information on subsets of cells within the larger population—the results obtained are simply the "average" of the population. This limitation is, perhaps, the critical failure of ektacytometry because, in many pathologic states, abnormal RBC represent a minor (<10%) fraction of the overall RBC mass hence subtle changes will not be clearly obvious. Moreover, it is difficult to recover RBC subsequent to ektacytometric analysis for further biologic testing due to the viscous media utilized and, using traditional ektacytometry, the fact that the RBC are irreversibly (in most cases) altered by the osmotic gradient employed during the assay.

2.3 Cell transit analysis

In contrast to micropipette analysis and ektacytometry, cell transit analysis provides information at both the single cell and populational level (**Figure 4**).

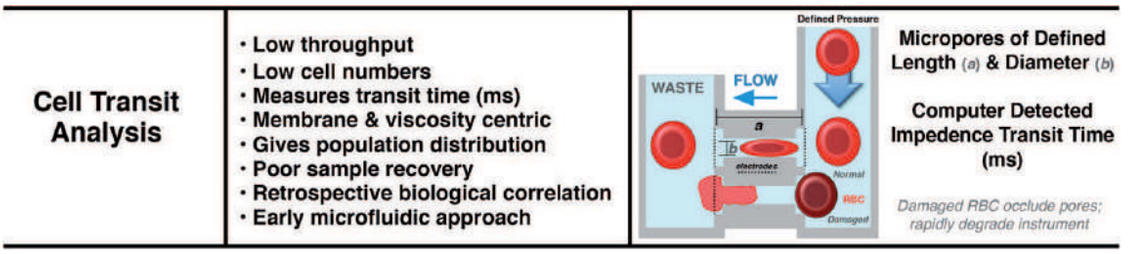

Figure 4.
Overview of cell transit analysis of blood cells. In contrast to micropipette analysis and ektacytometry, cell transit analysis provides information at both the single cell and populational level. Cellular deformability is indirectly measured via transit time (ms) of RBC through pores of defined diameter and length. Transit time is measured by the change in electrical resistance as an RBC passes through a micropore. Cell transit analysis is, in essence, an early micro (macro) fluidics approach.

To accomplish this, cell transit analysis combines features of both the traditional micropore filtration assay and the micropipette aspiration methodology, in that deformability of each RBC constitutes a single data point and can be used to then generate a populational distribution curve. In a cell transit analyzer, a single RBC passes through a micropore of fixed diameter and length with the transit time (in milliseconds; ms) of the cell calculated using the electrical resistance generated by the RBC within the channel as detected via a conductometer. However, the sensitivity of this method varies with cell size. Smaller cells, even if less deformable, pass through the pores with less resistance. In contrast, abnormally large or rigid cells, which are clinically important, are also be problematic as they block the micropore and are excluded from analysis [17, 69, 70]. Despite these limitations, cell transit analysis is very useful in that it provides subset/heterogeneity analysis via binning of the cells based on the transit time thus providing a continuous measure of the deformability profile of a sample and/or the severity of the deformability defect. The comparative utility of ektacytometry and cell transit analysis of RBC can be seen in normal and model ß thalassemic RBC in which purified alpha-hemoglobin chains are entrapped within normal RBC (**Figure 5**) [17, 19, 61–63]. While the ektacytometry and cell transit analysis have proven very useful as research tools, they have not been used to any great extent clinically. This is in large part due to the expense and complexity of the devices as well as their slow throughput making them impractical for clinical laboratories. Moreover, these in vitro studies often lack biological validation to the very low throughput of the assay (e.g., micropipette aspiration studies), overly small cell numbers, difficulty/impossibility of cell recovery post assessment, or more importantly, an inability to either identify or collect specific sample subsets (e.g., low versus high deformability) following analysis (e.g., Ektacytometry and Cell Transit Analysis studies).

2.4 Microfluidics

As noted in the preceding discussion, multiple micro/macro fluidic approaches have been used to model hemorheology of circulating blood cells; albeit almost exclusively RBC. Despite their valuable contributions to our understanding of blood cell deformability, these methods are inherently low throughput and dependent on relatively expensive instrumentation. But perhaps one of the biggest issues challenging these previous methodologies is the inability to recover substantial, or any, subpopulations (e.g., highly versus poorly deformable cells) from the analyzed sample. This weakness precludes additional in vitro or in vivo studies to tease out biological variations leading to the differential deformability profiles. Microfluidics approaches (**Figure 6**) potentially offers a cost-effective, high throughput,

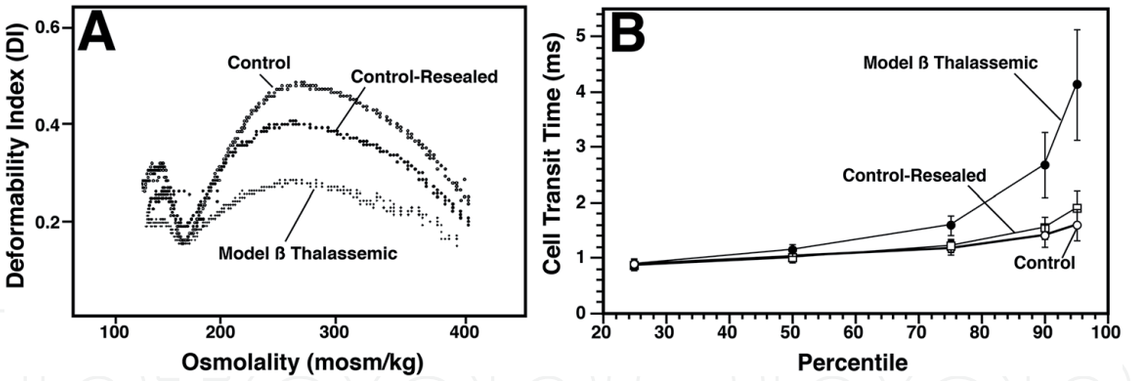

Figure 5.
Comparative data of normal versus model ß thalassemic RBC as assessed by ektacytometry and cell transit analysis. Panel A: as shown, ektacytometry provides the mean diffraction profile of a population of cells over a broad osmotic gradient; however, it does not provide any information as to the deformability distribution of the cells within the total population. Panel B: cell transit analysis gives information regarding both the deformability profile of the entire population and the individual cells within the tested population. Data derived from Refs. [17, 63].

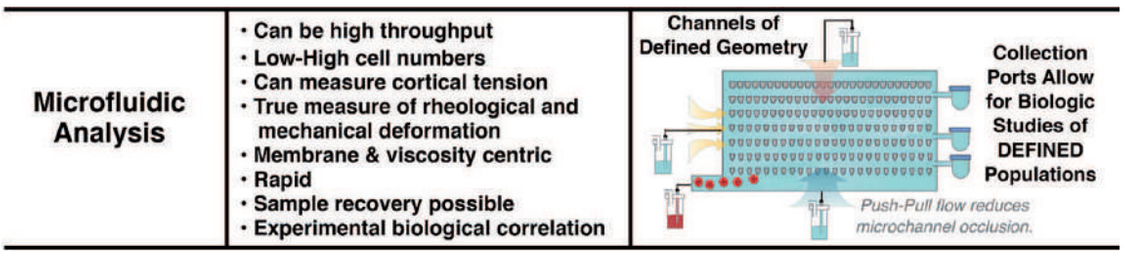

Figure 6.
Overview of microfluidic analysis of blood cells. Recent advances in microscale fabrication technologies have allowed for the development of an exceedingly broad array of microfluidic devices that may have utility in assessing the deformability of blood cells. These approaches range from single to multi-channel devices with channels of single or variable lengths and diameters. In addition, some designs incorporate collection ports so that cell exhibiting differential deformability profiles can be collected for further in vitro or in vivo study. Device shown is adapted from Guo et al. and Kang et al. [26, 28].

alternative to assessing blood cell deformability relative to these previous, and now rather ancient (as reflected by the key research papers relating to these approaches) technologies [22–25, 27, 28, 71–78]. Deformability measurement using microfluidics uses minute amounts of a whole blood or purified RBC/WBC in suspension flowing through a funnel-shaped micro-constriction(s) in a disposable plate. As demonstrated in our previous publications, and discussed in the following section, microfluidics devices are capable of providing reproducible intra- and inter-individual data, detecting oxidatively damaged RBC, identifying changes in RBC deformability consequent to storage, and identifying leukocytes [20–28].

3. Utility of microfluidics in transfusion medicine

As evidenced by the number of publications and patents being generated annually, the promise of microfluidic devices in medicine is seemingly unbounded. One area of particular interest to our laboratories has been in the field of transfusion medicine [20–28]. Annually over 100,000,000 units of blood are collected worldwide for transfusion purposes. Despite the volume collected, our tools for assessing the quality of the stored blood products remains primarily centered on 1950–80s technology. Upon collection of whole blood in Canada the blood is processed to produce 3 major components: RBC, platelets and plasma. The RBC component for

use in blood transfusion therapy are stored at 4°C for up to 42 days. The maximum storage window for RBC is based on studies dating from the 1950s on that defined a ≥ 75% recovery rate at 24 hours post-transfusion as the clinical "quality control" standard for stored donor RBC [79, 80]. Despite decades of research into RBC biology and advances in other aspects of transfusion medicine, the 24 hour survival rule remains the current gold standard for determining acceptable donor RBC quality in transfusion medicine. Currently there are no other established biomarkers by which blood services can discriminate "good" versus "bad" units. Note however, that ultimately the survival of the donor RBC is consequent to their vascular deformability (which is in turn governed by a multitude of biologic/metabolic factors). Hence, cost effectively assessing the deformability of stored RBC could serve as an excellent biomarker for the quality of stored donor RBC. Intriguingly, RBC deformability may also be a potent pre-screening tool that could be used to exclude potential donors from RBC donations. RBC which demonstrate poor initial deformability upon collection do not store well and may lead to adverse events in patients who receive these units. Poor deformability of potential donor RBC may arise from a broad range of issues including: undiagnosed RBC abnormalities (e.g., cytoskeletal, hemoglobin or metabolic aberrations); vascular inflammation; or dietary or drug-mediated alterations of the RBC.

To assess the deformability of blood cells, our laboratories have utilized a variety of microfluidic devices ranging from a simple, low throughput, funnel chain (prone to clogging) to a much more advanced and robust high throughput ratchet device. The ratchet microfluidic approach has proved better at assessing vascular deformability as blood cells are pushed laterally and vertically through tapered microchannels of decreasing size thus modeling the process of cellular deformation in microvasculature (**Figure 7**). Vertical movement is done via an oscillatory vertical pressure deferential that allows both a net vertical filtration flow and a downward declogging flow to minimize microchannel obstruction by blood cells as they reach their deformability limit. Importantly, this design also incorporates collection outlets allowing for recovery, and further testing, of cell populations with differential deformability profiles. Our research to date has demonstrated that this microfluidic microfiltration device is capable of isolating circulating tumor cells

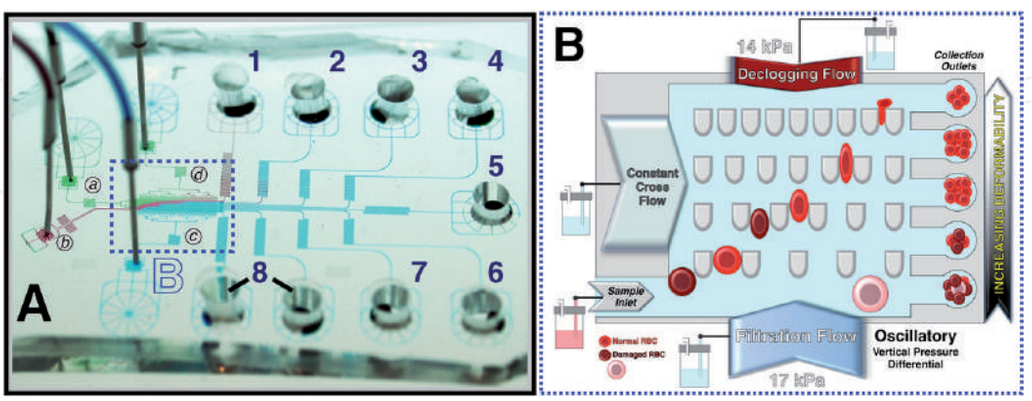

Figure 7.
General schematic of a ratchet microfluidic device. Panel A: shown is a photograph of the ratchet microfluidic device infused with different color dyes to highlight the design features: cross flow inlet (a), sample inlet (b), upward (c) and downward (d) oscillatory flow inlets, sorting region (dashed blue box) and outlets 1–8. In this design, outlets 8–1 corresponds to blocking pore sizes of ≥6.5, 5.5, 4.5, 4.0, 3.5, 3.0, 2.5 and 2.0 μm, respectively. Panel B: schematic of the sorting region showing the decreasing size of the tapered microchannels as well as the deformability of normal and oxidized RBC through these microchannels. Poorly deformable cells (e.g., oxidized RBC) are collected in outlets 8 and 7 while highly deformable cells are collected in outlets 3 thru 1. The downward oscillatory pressure minimizes channel obstruction by poorly deformable cells which are pushed horizontally into the collection outlets by the cross flow pressure. This device is suitable for use for both human RBC and WBC.

from leukocytes, malaria-infected and oxidized RBC from normal cells, granulocytes and lymphocytes from whole blood, and detecting early immune cell activation consequent to degranulation [26–28, 81].

Key to the use of microfluidic devices in RBC blood banking is documenting the ability of the device(s) to discriminate between "normal" and abnormal cellular deformability and document that the loss of deformability is associated with diminished in vivo circulation. Loss of cellular deformability can arise from a host of causes, most of which, due to the iron and oxygen rich environment of the RBC, leads to cellular oxidation [17–19, 23, 57, 61, 63, 82]. As shown in **Figure 8**, human or murine RBC oxidized by exposure to 50 μM phenazine methosulfate (PMS) were readily discriminated from normal RBC as measured by the cortical tension required to push the RBC through a funnel shaped micropore However, as noted by the differences between the human and murine RBC, the microchannel size (2–2.5 μm in this experiment) relative to the mean diameter of the RBC itself (~8 versus 6.7 μm for human and mouse RBC, respectively) will also play a role. Most importantly however, the loss of murine deformability in the oxidized RBC sample, as noted in the microfluidic device, correlated closely with the loss of in vivo survival. These findings suggest that microfluidic devices could prove useful for both diagnostic purposes (e.g., hemoglobinopathies such as sickle cell disease and thalassemia) as well as in evaluating the quality of stored human RBC prior to transfusion into a patient.

Indeed, microfluidics analysis of stored human RBC suggests that deformability is affected by storage time. As demonstrated by Matthews et al., using a microfluidic device, there is a significant loss of RBC deformability as early as 2 weeks into storage [25]. This finding confirms single-cell deformability studies that similarly

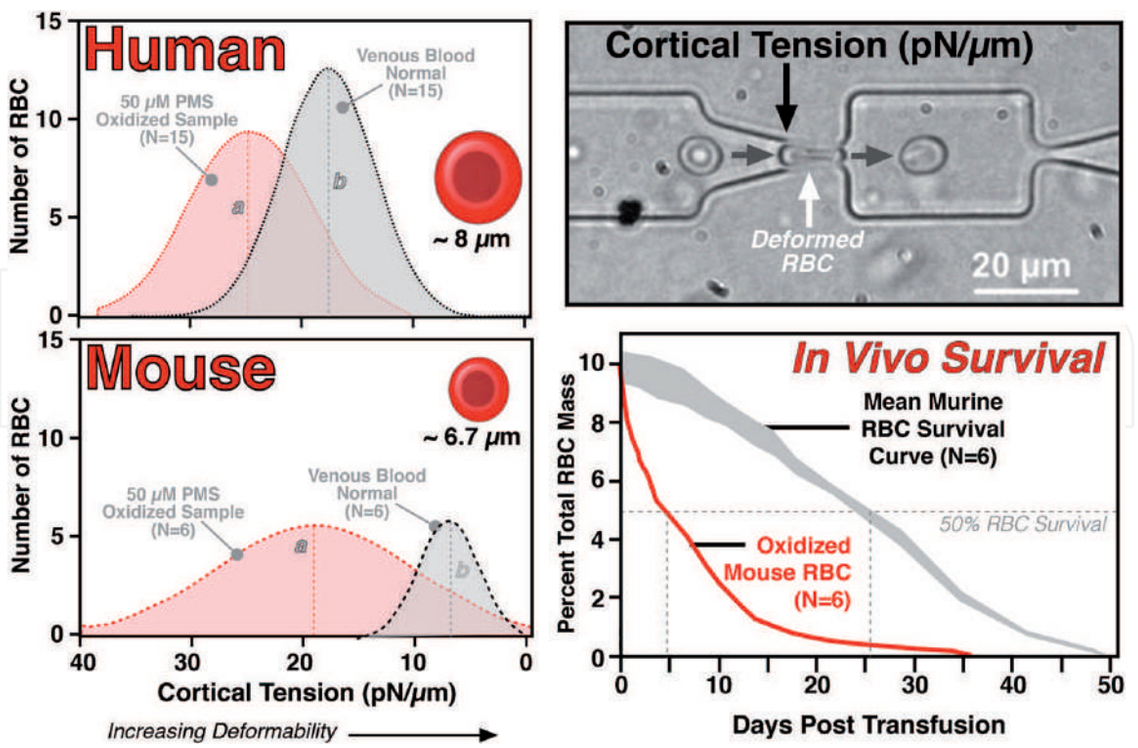

Figure 8.
Analysis of human and murine RBC deformability using a conical microfluidic array. The width of the funnel shaped micropore constriction used to measure RBC deformability was approximately 2–2.5 μm in size at its minimum. (a) and (b) equals peak count for oxidized and normal RBC respectively. Human blood was obtained via a finger prick while mouse blood was obtained by saphenous bleed. Also noted is the 50% in vivo survival point for oxidized (~5 days) and normal (~26 days) murine RBC. Data derived from Kwan et al. [23].

indicated that RBC deformability remained fairly constant in the first 2–3 weeks of storage and then rapidly decreased [83, 84]. However, in contrast to these single cell studies, our high throughput device can rapidly assess the proportion of individual RBCs that are too rigid to transit the microconstrictions and may, upon transfusion into an individual, be cleared by the spleen. Indeed, by day 42 of storage, 30% of all donor RBCs were too rigid to transit the device. Interestingly, a small subset of donors had RBC that demonstrated poor storage in that >50% of their RBC were too rigid to passage the microconstriction. These research findings suggest that the RBC quality of individual donors are, not unexpectedly, variable. The source of inter-individual variability causing the poor storage could be either inherent to the donor RBC itself (e.g., metabolic, structural or hemoglobin abnormalities) or transient (e.g., inflammation, food or drug induced).

The prescreening questionnaire completed by both new and repeat blood donors is focused, in part, on identifying factors that could adversely affect the quality of the blood product(s) produced from a donation. While most biologically-mediated RBC defects are likely to have been previously detected during normal medical surveillance of the prospective donor, transient inflammatory-mediated effects, such as those arising from viral, bacterial, drug or autoimmune events, are most likely to impact blood component quality. To address these potential risks, at the time of blood donation, all donors are asked if they feel ill or have had a recent fever. While the primary purpose of these self-reporting questions is to avoid transfusion of blood-borne infective agents or plasma that may contain potent immunomodulatory chemokines and cytokines, systemic inflammatory events may also result in bystander injury to the RBC that may compromise RBC storage and safety. The described microfluidics ratchet device may also provide a means of assessing both the WBC population and activation state of an individual [26, 28]. As shown in **Figure 9**, the ratchet microfluidic device described in **Figure 7**, is capable of differentially sorting monocytes from lymphocytes. The same device can also differentiate between resting (granule containing) from activated (degranulated) CD8+ T lymphocytes. Further refinement of the microchannel geometry will be capable of improving cell separation making it possible to readily prescreen individuals for evidence of immune activation thus improving blood component safety consequent to empirical donor evaluation versus self-reporting. Finally, microfluidic devices

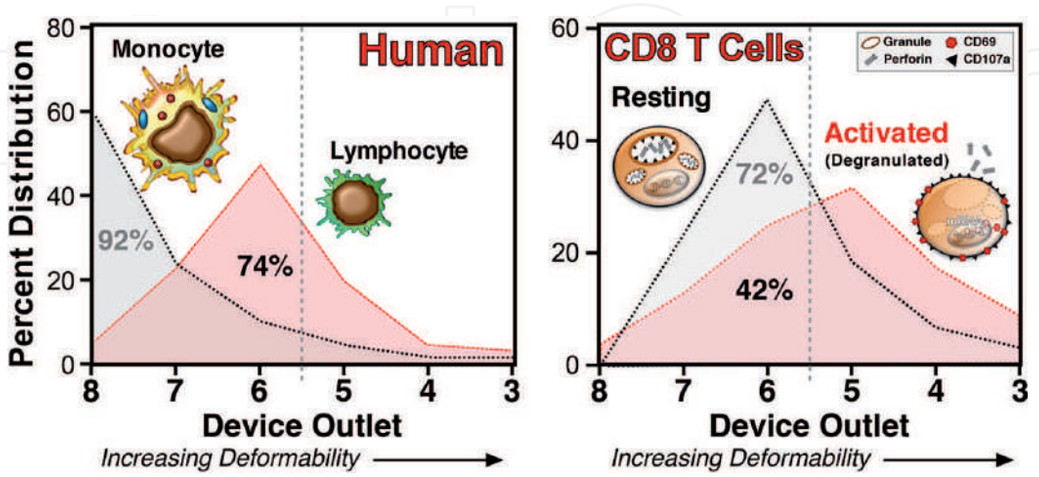

Figure 9.
Analysis of human monocyte and lymphocyte populations showing differential sorting on the ratchet microfluidic device. Note that the prototype device can also detect degranulation of lymphocytes (shown are CD8+ T cells) which occurs upon inflammatory activation. The vertical dashed line separates cells based on less deformable (collection outlets 8–6) and more deformable (collection outlets 5–3). Data derived from Kang et al. [28].

could also be used during the blood collection process, as well as in the field, to screen individuals who have reported recent travel to malarial endemic areas, for actual malaria infection [27, 85–88]. Currently, individuals traveling to malarial endemic regions are deferred from blood donation; an action that often results in their permanent loss from the blood donor pool.

4. Conclusions

Microfluidics devices have the potential to dramatically, and cost-effectively, change the practice of transfusion medicine. As illustrated, purpose-specific development of ratchet microfluidics devices will make it possible, via a finger prick (e.g., as shown in **Figure 8**), to prescreen donors at the time of pre-donation testing (i.e., simultaneously with determining the donor's hematocrit prior to unit donation) to select donors whose RBC show normal deformability profiles prior to storage. Donors with RBC deformability profiles outside of the normal range would be deferred from RBC donation, though potentially, still donating plasma for fractionation into plasma protein components. Moreover, the same microfluidic approach could improve the detection of patients with recent/current systemic immune activation that could result in the presence of undesirable cytokines/chemokines within the donated blood or that might have adversely affected normal RBC deformability. Hence, the cost-effective microfluidic-based prescreening process would potentially diminish the risk to patient safety that accompanies ineffectual RBC transfusion and/or the presence of inflammatory mediators in blood products. Not inconsequentially, prescreening for good donors would reduce the expense to the blood operator associated with the production and distribution of a potentially ineffectual, or unsafe, blood unit. Beyond prescreening donors, patient safety would also be enhanced by doing point-of-care deformability analysis of stored RBC prior to transfusion. Such analysis would enhance patient safety by reducing the aggregate transfusion needs of a patient by preventing the transfusion of RBC which would have poor in vivo survivability. Such an approach would be of particular value in the chronically transfused patient (e.g., sickle cell, thalassemic and myelodysplastic) populations.

Acknowledgements

This work was supported by grants from the Canadian Institutes of Health Research (325,373, HM and MDS, 322375, HM; and 362,500, HM), Canadian Blood Services-CIHR Partnership program (BUC21403-HM; HM and MDS), Canadian Blood Services (MDS) and Health Canada (MDS). The views expressed herein do not necessarily represent the view of the federal government of Canada. We thank the Canada Foundation for Innovation and the Michael Smith Foundation for Health Research for infrastructure funding at the University of British Columbia Centre for Blood Research. The funders had no role in study design, data collection and analysis, decision to publish, or preparation of the manuscript.

Conflict of interest

The University of British Columbia and HM have pending patent applications relating to the described microfluidic devices.

Author details

Mark D. Scott[1,2,3*], Kerryn Matthews[2,4] and Hongshen Ma[2,4]

1 Centre for Innovation, Canadian Blood Services, University of British Columbia, Vancouver, BC, Canada

2 Centre for Blood Research, University of British Columbia, Vancouver, BC, Canada

3 Department of Pathology and Laboratory Medicine, University of British Columbia, Vancouver, BC, Canada

4 Department of Mechanical Engineering, University of British Columbia, Vancouver, BC, Canada

*Address all correspondence to: mdscott@mail.ubc.ca

References

[1] Aird WC. Spatial and temporal dynamics of the endothelium. Journal of Thrombosis and Haemostasis. 2005;**3**:1392-1406

[2] Wexler L, Bergel DH, Gabe IT, Makin GS, Mills CJ. Velocity of blood flow in normal human venae cavae. Circulation Research. 1968;**23**:349-359

[3] Weiss L, Tavassoli M. Anatomical hazards to the passage of erythrocytes through the spleen. Seminars in Hematology. 1970;**7**:372-380

[4] Chen LT, Weiss L. The role of the sinus wall in the passage of erythrocytes through the spleen. Blood. 1973;**41**:529-537

[5] LaCelle PL. Alteration of membrane deformability in hemolytic anemias. Seminars in Hematology. 1970;**7**:355-371

[6] Weed RI. The importance of erythrocyte deformability. The American Journal of Medicine. 1970;**49**:147-150

[7] Chien S, Usami S, Bertles JF. Abnormal rheology of oxygenated blood in sickle cell anemia. The Journal of Clinical Investigation. 1970;**49**:623-634

[8] Chien S, Usami S, Dellenback RJ, Gregersen MI. Shear-dependent deformation of erythrocytes in rheology of human blood. The American Journal of Physiology. 1970;**219**:136-142

[9] Bessis M, Mohandas N. Red cell structure, shapes and deformability. British Journal of Haematology. 1975;**31**:5-11

[10] La Celle PL. Pathogenic erythrocytes in the capillary microcirculation. Blood Cells. 1975;**1**:269-284

[11] Havell TC, Hillman D, Lessin LS. Deformability characteristics of sickle cells by microelastimetry. American Journal of Hematology. 1978;**4**:9-16

[12] Mohandas N, Phillips WM, Bessis M. Red blood cell deformability and hemolytic anemias. Seminars in Hematology. 1979;**16**:95-114

[13] Clark MR, Mohandas N, Shohet SB. Deformability of oxygenated irreversibly sickled cells. The Journal of Clinical Investigation. 1980;**65**:189-195

[14] Clark MR, Mohandas N, Shohet SB. Osmotic gradient ektacytometry: Comprehensive characterization of red cell volume and surface maintenance. Blood. 1983;**61**:899-910

[15] Snyder LM, Fortier NL, Trainor J, Jacobs J, Leb L, Lubin B, et al. Effect of hydrogen peroxide exposure on normal human erythrocyte deformability, morphology, surface characteristics, and spectrin-hemoglobin cross-linking. The Journal of Clinical Investigation. 1985;**76**:1971-1977

[16] Snyder LM, Fortier NL, Leb L, McKenney J, Trainor J, Sheerin H, et al. The role of membrane protein sulfhydryl groups in hydrogen peroxide-mediated membrane damage in human erythrocytes. Biochimica et Biophysica Acta. 1988;**937**:229-240

[17] Scott MD, Rouyer-Fessard P, Ba MS, Lubin BH, Beuzard Y. Alpha- and beta-haemoglobin chain induced changes in normal erythrocyte deformability: Comparison to beta thalassaemia intermedia and Hb H disease. British Journal of Haematology. 1992;**80**:519-526

[18] Scott MD, van den Berg JJ, Repka T, Rouyer-Fessard P, Hebbel RP, Beuzard Y, et al. Effect of excess alpha-hemoglobin chains on cellular and membrane oxidation in model beta-thalassemic erythrocytes. The Journal of Clinical Investigation. 1993;**91**:1706-1712

[19] Scott MD. H2O2 injury in beta thalassemic erythrocytes: Protective role of catalase and the prooxidant effects of GSH. Free Radical Biology & Medicine. 2006;**40**:1264-1272

[20] Guo Q, McFaul SM, Ma H. Deterministic microfluidic ratchet based on the deformation of individual cells. Physical Review E, Statistical, Nonlinear, and Soft Matter Physics. 2011;**83**:051910

[21] Guo Q, Reiling SJ, Rohrbach P, Ma H. Microfluidic biomechanical assay for red blood cells parasitized by plasmodium falciparum. Lab on a Chip. 2012;**12**:1143-1150

[22] Guo Q, Park S, Ma H. Microfluidic micropipette aspiration for measuring the deformability of single cells. Lab on a Chip. 2012;**12**:2687-2695

[23] Kwan JM, Guo Q, Kyluik-Price DL, Ma H, Scott MD. Microfluidic analysis of cellular deformability of normal and oxidatively damaged red blood cells. American Journal of Hematology. 2013;**88**:682-689

[24] Guo Q, Duffy SP, Matthews K, Santoso AT, Scott MD, Ma H. Microfluidic analysis of red blood cell deformability. Journal of Biomechanics. 2014;**47**:1767-1776

[25] Matthews K, Myrand-Lapierre ME, Ang RR, Duffy SP, Scott MD, Ma H. Microfluidic deformability analysis of the red cell storage lesion. Journal of Biomechanics. 2015;**48**:4065-4072

[26] Guo Q, Duffy SP, Matthews K, Islamzada E, Ma H. Deformability based cell sorting using microfluidic ratchets enabling phenotypic separation of leukocytes directly from whole blood. Scientific Reports. 2017;**7**:6627

[27] Matthews K, Duffy SP, Myrand-Lapierre ME, Ang RR, Li L, Scott MD, et al. Microfluidic analysis of red blood cell deformability as a means to assess hemin-induced oxidative stress resulting from plasmodium falciparum intraerythrocytic parasitism. Integrative Biology. 2017;**9**:519-528

[28] Kang N, Guo Q, Islamzada E, Ma H, Scott MD. Microfluidic determination of lymphocyte vascular deformability: Effects of intracellular complexity and early immune activation. Integrative Biology. 2018;**10**:207-217

[29] Abbas AK, Lichtman AH, Pillai S. Cellular and Molecular Immunology. Philadelphia, Pennsylvania, USA: Elsevier/Saunders; 2014:13-34

[30] Rosenbluth MJ, Lam WA, Fletcher DA. Force microscopy of nonadherent cells: A comparison of leukemia cell deformability. Biophysical Journal. 2006;**90**:2994-3003

[31] Mege JL, Capo C, Benoliel AM, Foa C, Bongrand P. Study of cell deformability by a simple method. Journal of Immunological Methods. 1985;**82**:3-15

[32] Pasternak C, Elson EL. Lymphocyte mechanical response triggered by cross-linking surface receptors. The Journal of Cell Biology. 1985;**100**:860-872

[33] Downey GP, Doherty DE, Schwab B, Elson EL, Henson PM, Worthen GS. Retention of leukocytes in capillaries: Role of cell size and deformability. Journal of Applied Physiology. 1990;**69**:1767-1778

[34] Brown MJ, Hallam JA, Colucci-Guyon E, Shaw S. Rigidity of circulating lymphocytes is primarily conferred by vimentin intermediate filaments. Journal of Immunology. 2001;**166**:6640-6646

[35] Esteban-Manzanares G, González-Bermúdez B, Cruces J, De la Fuente M, Li Q, Guinea GV, et al.

Improved measurement of elastic properties of cells by micropipette aspiration and its application to lymphocytes. Annals of Biomedical Engineering. 2017;**45**:1375-1385

[36] Zhang X, Cook PC, Zindy E, Williams CJ, Jowitt TA, Streuli CH, et al. Integrin α4β1 controls G9a activity that regulates epigenetic changes and nuclear properties required for lymphocyte migration. Nucleic Acids Research. 2016;**44**:3031-3044

[37] Nevaril CG, Lynch EC, Alfrey CP, Hellums JD. Erythrocyte damage and destruction induced by shearing stress. The Journal of Laboratory and Clinical Medicine. 1968;**71**:784-790

[38] La Celle PL. Alteration of deformability of the erythrocyte membrane in stored blood. Transfusion. 1969;**9**:238-245

[39] Weed RI, LaCelle PL, Merrill ET. Erythrocyte metabolism and cellular deformability. Vox Sanguinis. 1969;**17**:32-33

[40] Weed RI, LaCelle PL, Merrill EW. Metabolic dependence of red cell deformability. The Journal of Clinical Investigation. 1969;**48**:795-809

[41] Evans E, Mohandas N, Leung A. Static and dynamic rigidities of normal and sickle erythrocytes. Major influence of cell hemoglobin concentration. The Journal of Clinical Investigation. 1984;**73**:477-488

[42] Evans EA, Mohandas N. Membrane-associated sickle hemoglobin: A major determinant of sickle erythrocyte rigidity. Blood. 1987;**70**:1443-1449

[43] Ballas SK, Larner J, Smith ED, Surrey S, Schwartz E, Rappaport EF. Rheologic predictors of the severity of the painful sickle cell crisis. Blood. 1988;**72**:1216-1223

[44] Mohandas N, Evans E. Mechanical properties of the red cell membrane in relation to molecular structure and genetic defects. Annual Review of Biophysics and Biomolecular Structure. 1994;**23**:787-818

[45] Discher DE, Mohandas N, Evans EA. Molecular maps of red cell deformation: Hidden elasticity and in situ connectivity. Science. 1994;**266**:1032-1035

[46] Heinrich V, Ritchie K, Mohandas N, Evans E. Elastic thickness compressibilty of the red cell membrane. Biophysical Journal. 2001;**81**:1452-1463

[47] Evans J, Gratzer W, Mohandas N, Parker K, Sleep J. Fluctuations of the red blood cell membrane: Relation to mechanical properties and lack of ATP dependence. Biophysical Journal. 2008;**94**:4134-4144

[48] Schmid-Schönbein GW, Sung KL, Tözeren H, Skalak R, Chien S. Passive mechanical properties of human leukocytes. Biophysical Journal. 1981;**36**:243-256

[49] Derganc J, Bozic B, Svetina S, Zeks B. Stability analysis of micropipette aspiration of neutrophils. Biophysical Journal. 2000;**79**:153-162

[50] Shao JY, Xu J. A modified micropipette aspiration technique and its application to tether formation from human neutrophils. Journal of Biomechanical Engineering. 2002;**124**:388-396

[51] Liu B, Goergen CJ, Shao JY. Effect of temperature on tether extraction, surface protrusion, and cortical tension of human neutrophils. Biophysical Journal. 2007;**93**:2923-2933

[52] Kaleridis V, Athanassiou G, Deligianni D, Missirlis Y. Slow flow of passive neutrophils and sequestered nucleus into micropipette. Clinical

Hemorheology and Microcirculation. 2010;**45**:53-65

[53] Guillou L, Babataheri A, Saitakis M, Bohineust A, Dogniaux S, Hivroz C, et al. T-lymphocyte passive deformation is controlled by unfolding of membrane surface reservoirs. Molecular Biology of the Cell. 2016;**27**:3574-3582

[54] Kuypers FA, Chiu D-Y, Mohandas N, Roelofsen B, Op den Kamp JAF, Lubin BH. The molecular species composition of phosphatidylcholine affects cellular properties in normal and sickle erythrocytes. Blood. 1987;**70**:1111-1118

[55] Green MA, Noguchi CT, Keidan AJ, Marwah SS, Stuart J. Polymerization of sickle cell hemoglobin at arterial oxygen saturation impairs erthrocyte deformability. The Journal of Clinical Investigation. 1988;**81**:1669-1674

[56] Chasis JA, Schrier SL. Membrane deformability and the capacity for shape change in the erythrocyte. Blood. 1989;**74**:2562-2568

[57] Kuypers FA, Scott MD, Schott MA, Lubin B, Chiu DT. Use of ektacytometry to determine red cell susceptibility to oxidative stress. The Journal of Laboratory and Clinical Medicine. 1990;**116**:535-545

[58] Scott MD, Meshnick SR, Williams RA, Chiu D-Y, Lubin FA, Kuypers FA. Qinghaosu-enhanced oxidant sensitivity in erythrocytes with unstable hemoglobins. Blood. 1988;**72**:200

[59] Scott MD, Eaton JW, Kuypers FA, Chiu D-Y, Lubin BH. Enhancement of erythrocyte superoxide dismutase activity: Effects on cellular oxidant defense. Blood. 1989;**74**:2542-2549

[60] Butikofer P, Lin ZW, Kuypers FA, Scott MD, Xu CM, Wagner GM, et al. Chlorpromazine inhibits vesiculation, alters phosphoinositide turnover and changes deformability of ATP-depleted RBCs. Blood. 1989;**73**:1699-1704

[61] Scott MD, Rouyer-Fessard P, Lubin BH, Beuzard Y. Entrapment of purified alpha-hemoglobin chains in normal erythrocytes. A model for beta thalassemia. The Journal of Biological Chemistry. 1990;**265**:17953-17959

[62] Scott MD, Kuypers FA, Butikofer P, Bookchin RM, Ortiz OE, Lubin BH. Effect of osmotic lysis and resealing on red cell structure and function. The Journal of Laboratory and Clinical Medicine. 1990;**115**:470-480

[63] Kuypers FA, Schott MA, Scott MD. Phospholipid composition and organization in model beta-thalassemic erythrocytes. American Journal of Hematology. 1996;**51**:45-54

[64] Murad KL, Mahany KL, Brugnara C, Kuypers FA, Eaton JW, Scott MD. Structural and functional consequences of antigenic modulation of red blood cells with methoxypoly(ethylene glycol). Blood. 1999;**93**:2121-2127

[65] Streekstra GJ, Dobbe JG, Hoekstra AG. Quantification of the fraction poorly deformable red blood cells using ektacytometry. Optics Express. 2010;**18**:14173-14182

[66] Frank SM, Abazyan B, Ono M, Hogue CW, Cohen DB, Berkowitz DE, et al. Decreased erythrocyte deformability after transfusion and the effects of erythrocyte storage duration. Anesthesia and Analgesia. 2013;**116**:975-981

[67] Reinhart WH, Piety NZ, Deuel JW, Makhro A, Schulzki T, Bogdanov N, et al. Washing stored red blood cells in an albumin solution improves their morphologic and hemorheologic properties. Transfusion. 2015;**55**:1872-1881

[68] Nagababu E, Scott AV, Johnson DJ, Dwyer IM, Lipsitz JA, Barodka VM, et al. Oxidative stress and rheologic properties of stored red blood cells before and after transfusion to surgical patients. Transfusion. 2016;**56**:1101-1111

[69] Baskurt OK. Deformability of red blood cells from different species studied by resistive pulse shape analysis technique. Biorheology. 1996;**33**:169-179

[70] OK B, TC F, HJ M. Sensitivity of the cell transit analyzer (CTA) to alterations of red blood cell deformability: Role of cell size-pore size ratio and sample preparation. Clinical Hemorheology. 1996;**16**:753-765

[71] Whitesides GM. The origins and the future of microfluidics. Nature. 2006;**442**:368-373

[72] Shevkoplyas SS, Yoshida T, Gifford SC, Bitensky MW. Direct measurement of the impact of impaired erythrocyte deformability on microvascular network perfusion in a microfluidic device. Lab on a Chip. 2006;**6**:914-920

[73] Xia N, Hunt TP, Mayers BT, Alsberg E, Whitesides GM, Westervelt RM, et al. Combined microfluidic-micromagnetic separation of living cells in continuous flow. Biomedical Microdevices. 2006;**8**:299-308

[74] Bransky A, Korin N, Nemirovski Y, Dinnar U. Correlation between erythrocytes deformability and size: A study using a microchannel based cell analyzer. Microvascular Research. 2007;**73**:7-13

[75] Forsyth AM, Wan J, Ristenpart WD, Stone HA. The dynamic behavior of chemically "stiffened" red blood cells in microchannel flows. Microvascular Research. 2010;**80**:37-43

[76] Ye T, Li H, Lam KY. Modeling and simulation of microfluid effects on deformation behavior of a red blood cell in a capillary. Microvascular Research. 2010;**80**:453-463

[77] Martin JD, Marhefka JN, Migler KB, Hudson SD. Interfacial rheology through microfluidics. Advanced Materials. 2011;**23**:426-432

[78] Patel KV, Mohanty JG, Kanapuru B, Hesdorffer C, Ershler WB, Rifkind JM. Association of the red cell distribution width with red blood cell deformability. Advances in Experimental Medicine and Biology. 2013;**765**:211-216

[79] Bratosin D, Estaquier J, Ameisen JC, Montreuil J. Molecular and cellular mechanisms of erythrocyte programmed cell death: Impact on blood transfusion. Vox Sanguinis. 2002;**83**(Suppl. 1):307-310

[80] Dumont LJ, AuBuchon JP. Evaluation of proposed FDA criteria for the evaluation of radiolabeled red cell recovery trials. Transfusion. 2008;**48**:1053-1060

[81] Park ES, Jin C, Guo Q, Ang RR, Duffy SP, Matthews K, et al. Continuous flow deformability-based separation of circulating tumor cells using microfluidic ratchets. Small. 2016;**12**:1909-1919

[82] Scott MD, Eaton JW. Thalassaemic erythrocytes: Cellular suicide arising from iron and glutathione-dependent oxidation reactions. British Journal of Haematology. 1995;**91**:811-819

[83] Czerwinska J, Rieger M, Uehlinger DE. Dynamics of red blood cells in microporous membranes. Biomicrofluidics. 2014;**8**:044101

[84] Huang S, Hou HW, Kanias T, Sertorio JT, Chen H, Sinchar D, et al. Towards microfluidic-based depletion of stiff and fragile human red cells that

accumulate during blood storage. Lab on a Chip. 2015;**15**:448-458

[85] Santoso AT, Deng X, Lee JH, Matthews K, Duffy SP, Islamzada E, et al. Microfluidic cell-phoresis enabling high-throughput analysis of red blood cell deformability and biophysical screening of antimalarial drugs. Lab on a Chip. 2015;**15**:4451-4460

[86] Myrand-Lapierre ME, Deng X, Ang RR, Matthews K, Santoso AT, Ma H. Multiplexed fluidic plunger mechanism for the measurement of red blood cell deformability. Lab on a Chip. 2015;**15**:159-167

[87] Deng X, Duffy SP, Myrand-Lapierre ME, Matthews K, Santoso AT, Du YL, et al. Reduced deformability of parasitized red blood cells as a biomarker for anti-malarial drug efficacy. Malaria Journal. 2015;**14**:428

[88] Guo Q, Duffy SP, Matthews K, Deng X, Santoso AT, Islamzada E, et al. Deformability based sorting of red blood cells improves diagnostic sensitivity for malaria caused by plasmodium falciparum. Lab on a Chip. 2016;**16**:645-654